J Fluoresc (2012) 22:971–992
DOI 10.1007/s10895-011-1036-7

ORIGINAL PAPER

Fluorescence and Electrochemical Recognition of Nucleosides and DNA by A Novel Luminescent Bioprobe Eu(lll) -TNB

Hassan A. Azab · E. M. Mogahed · F. K. Awad · R. M. Abd El Aal · Rasha M. Kamel

Received: 24 November 2011 / Accepted: 28 December 2011 / Published online: 3 February 2012

Abstract The luminescence arising from lanthanide cations offers several advantages over organic fluorescent molecules: sharp, distinctive emission bands allow for easy resolution between multiple lanthanide signals; long emission lifetimes (μs –ms) make them excellent candidates for time-resolved measurements; and high resistance to photo bleaching allow for long or repeated experiments. A method is presented for determination of nucleosides using the effect of enhancement of fluorescence of the easily accessible europium(III)-TNB in presence of different nucleosides. The latter coordinates to Eu(III) -TNB and enhances its luminescence intensity as a result of the displacement of water from the inner coordination sphere of the central metal. A similar method for the determination of DNA based on the quenching of Eu(III)-TNB has been established. The interaction of Eu(III)-4,4,4 trifluoro-1-(2-naphthyl)1,3-butanedione (TNB) complex with nucleosides (NS) (guanosine, adenosine, cytidine , inosine) and DNA has been studied using normal and time-resolved luminescence techniques. Binding constants were determined at 293 K, 298 K, 303 K, 308 K and 313 K by using Benesi-Hildebrand equation. A thermodynamic analysis showed that the reaction is spontaneous with ΔG being negative. The enthalpy ΔH and the entropy ΔS of reactions were all determined. The formation of binary and ternary complexes of Eu (III) with nucleosides and TNB has been studied potentiometrically at (25.0±0.1) °C and ionic strength I=0.1 mol.dm^{-3} (KNO_3) . The formation of the 1:1 binary and 1:1:1 ternary complexes are inferred from the corresponding titration curves. Initial estimates of the formation constants of the resulting species and the protonation constants of the different ligands used have been refined with the HYPERQUAD computer program. Electrochemical investigations for the systems under investigations have been carried out using cyclic voltammetry (CV), differential pulse polarography (DPP), and square wave voltammetry (SWV) on a glassy carbon electrode in I=0.1 mol/L p-toluenesulfonate as supporting electrolyte.

Keywords Europium-TNB · Adenosine · Guanosine · Cytidine · Inosine · DNA · Time-resolved luminescence · Voltammetry · Glassy carbon electrode

H. A. Azab (✉)
Chemistry Department faculty of science, Suez Canal University, Ismailia 41522, Egypt
e-mail: azab2@yahoo.com

E. M. Mogahed · F. K. Awad · R. M. A. El Aal · R. M. Kamel
Chemistry Department, Faculty of Science, Suez Canal University, Suez, Egypt

E. M. Mogahed
e-mail: emmsaad@yahoo.com

F. K. Awad
e-mail: awadpoll@yahoo.com

R. M. A. El Aal
e-mail: abdelal2001@yahoo.com

R. M. Kamel
e-mail: rashamoka@yahoo.com

Introduction

Deoxyribonucleic acid (DNA) is the primary target molecule for most anticancer and antiviral therapies according to cell biology [1, 2]. Investigations of the interaction between small molecules and DNA are basic work in the design of new types of pharmaceutical molecules. Small molecule which can interact with DNA has been divided into several categories: metal ion and metal complex, such as metal bipyridyl complex [3] and metal phenanthroline complex

[4]; heavy metal which causes the damage of DNA such as chromium [5]; antibiotics, organic dye and organic pesticide [6, 7]; protein molecule; nanoparticles marker [8]. Small molecules have been studied extensively, due to their utility in the design and development of synthetic restriction enzymes, new drugs, DNA footprinting agents and as the probe of DNA structure.

The quantitative analysis of DNA is very important because it is often used as a reference for measurements of other components in biological samples. Several methods have been developed based on spectroscopy [9], chemiluminescence [10], resonance light scattering [11], fluorescence [12], phosphorescence [13], chromatography [14] and electrochemical [15] techniques for sensing of DNA. Direct use of the natural fluorescence emission properties of DNA for their structure, dynamic studies, and fluorimetric determinations has been limited, which is due to the low fluorescence quantum yield of native DNA.

Purine and pyrimidine derivatives have great importance in nature. In particular, the nucleotides of adenine and guanine together with those of thymine and cytosine represent the monomer units of nucleic acids. Dietary purines, including nucleotides, nucleosides and bases, are reported to be absorbed as the corresponding nucleosides or bases and are utilized through the purine metabolic pathway [16–20]. The end product of purine metabolism is uric acid and the increase of serum uric acid level causes gout and hyperuricemia [16, 21]. Serum uric acid levels in individuals who regularly consume purine-rich foods are reported to be higher than in those who consume less of these foods [22]. Patients with gout tend to consume large amounts of meat or giblets, which contain high levels of purine [23, 24]. Although there have been many reports investigating the effects of food on purine metabolism and serum uric acid levels [17, 19, 24–26], few reports [27] have examined the amounts of individual purine nucleosides, nucleotides, bases and nucleic acids in food. Because purine nucleotides, nucleosides and bases exert different effects on serum uric acid levels [28], it is necessary to examine the levels of individual nucleosides, nucleotides, bases and nucleic acids in various foods in order to investigate the effects of purine-rich foods on the elevation of serum uric acid levels.

Several methods have been reported for the determination of nucleoside and nucleotide concentrations in cells [29–33], biological samples [34, 35] or milk [36]. High-performance liquid chromatography (HPLC) [34, 36], liquid chromatography–mass spectrometry (LC–MS) [29–31, 35], and LC/MS/MS [32, 33, 37] have been used for such measurements. However, the simultaneous determination of inosine, IMP, uridine, thymidine and cytidine has not been performed to date. It was thus considered to be necessary to develop a method for quantifying purine and pyrimidine nucleosides and nucleotides including these compounds.

The use of lanthanide chelates as luminescent indicators, rather than conventional fluorophores, can enable highly sensitive detection due to their specific properties. In particular, the large Stokes' shift of lanthanide chelates (mostly Eu^{3+} and Tb^{3+}) easily permits selection of the chelate-specific emission from scattered excitation light, even with filters. The narrow emission bands allow efficient separation of several luminescence signals in multicolor assays. Further, the very long luminescence life time permits gated detection on a micro- to millisecond timescale to avoid typical short-lived non-specific background signals [38, 39].In these systems, intense ion luminescence originates from the intramolecular energy transfer from the excited triplet-state of the ligand to the emitting level of the lanthanide (antenna effect) [40]. A new strategy for CT-DNA hybridization can be suggested using Eu(III)-TNB as fluorescence probe. Furthermore, this label-free method for CT-DNA hybridization detection can avoid the laborious labeling or modifying steps, which can make the process simple, rapid, and low in cost; the hybridization and detection are performed in homogeneous solution without steric constraints. Herein, the aim of the present study is to examine the interaction of Eu(III) with TNB and nucleosides adenosine, guanosine, cytidine, inosine and with DNA. The present study can be considered as a continuation for the author work in the field of analytical applications of lanthanide complexes [41–50].

Experimental

Chemicals

Europium chloride hexahydrate ($EuCl_3.6H_2O$) was purchased from Sigma-Aldrich, DNA and nucleosides under study (Scheme 1) adenosine, guanosine, cytidine and inosine were from Sigma-Aldrich. 4,4,4 trifluoro-1-(2-naphthyl)1,3-butanedione (TNB) was from Merck and ethanol used is of analytical grade quality from Sigma-Aldrich.

Stock Solutions

Stock solution of $EuCl_3.6H_2O$ was prepared by dissolving 36.6 mg in 100 ml deionized water to give a final concentration of 10^{-3} mol/L. For a stock solution of 10^{-3} mol/L of the ligand (TNB) 26.6 mg of solid ligand were dissolved in 100 ml of ethanol. The stock solutions of 10^{-3} mol/L of nucleosides were prepared by dissolving 26.7, 28.3, 24.3 and 26.8 mg,respectively in deionized water for adenosine, guanosine, cytidine and inosine. The working solution of Eu^{3+}, TNB, DNA and nucleosides were prepared daily by dilution of the stock solutions in deionized water.

Scheme 1 Chemical structure of Nucleosides under study and TNB

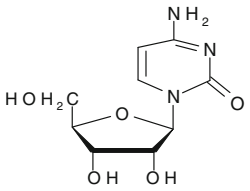

Cytidine (4-amino-1- β-D-ribofuranosyl-2-(1H)-pyrimidine)

($C_9H_{13}N_3O_5$)

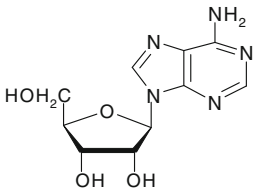

Adenosine (9-β-D-ribfuranosyl-9H-purine-6-amine)

(9-β-D-ribofuranosyl-adenine)

($C_{10}H_{13}N_5O_4$)

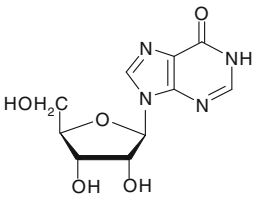

Inosine (1,9-dihydro-9-β-D-ribfuranosyl-6H-purine-6-one)

(Hypoxanthine-9-D-ribofuranoside)

($C_{10}H_{12}N_4O_5$)

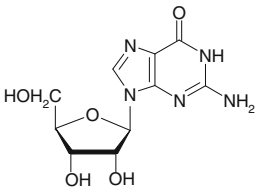

Guanosine (2-amino-1,9-dihydro-9-β-D-ribfuranosyl-6H-purine-6-one)

(9-β-D-ribofuranosyl-guanine)

($C_{10}H_{13}N_5O_5$)

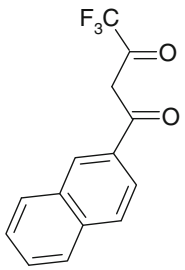

4,4,4 trifluoro-1-(2-naphthyl)1,3-butanedione (TNB).

Methods

A 10 ml solution containing appropriate concentration of 1×10^{-5} M $EuCl_3.6H_2O$ and 2×10^{-5} M TNB was added to 1×10^{-5} M nucleoside solutions and mixed using a magnetic stirrer for about ten minutes. UV-visible spectra of all solutions were recorded in the range of 200–400nm.

A known concentration of $EuCl_3.6H_2O$ and TNB in Tris-HCl solution was added into 1×10^{-6} M DNA and 1×10^{-5} M nucleosides and were mixed at different temperatures. The fluorescent intensity of the solution was recorded at excitation wavelength of 340 nm by using A JASCO-FP6300 spectrofluorometer and kept at 25±1 °C for 10 min. Luminescence intensity was measured in a 1 cm quartz cell at an excitation wavelength of 340 nm and an emission wavelength of 614 nm, 150 μL of each solution were pipetted into a 96-well microtiterplate (each of 12 columns contained different concentrations of DNA or nucleosides under study with eight replicates of the same concentration) and the time-resolved luminescence intensities were measured in a microtiterplate reader.

For potentiometric measurements a CO_2 free solution of potassium hydroxide (Merck AG) was prepared and standardized against multiple samples of primary standard potassium hydrogen phthalate (Merck AG) . HNO_3 solutions were prepared and standardized potentiometrically with tris (hydroxyl methyl) amino methane. The ionic strength of the studied solutions was adjusted to 0.1 mol.dm^{-3} using a stock solution of KNO_3 in potentiometric and spectral measurements. KNO_3 was from Merck AG. In electroanalytical measurements, the ionic strength of the examined solutions was adjusted to 0.1 mol.dm^{-3} using an alcoholic solution of p-toluenesulfonate. This supporting electrolyte was purchased from Merck AG.

Instruments

Luminescence time –resolved measurements in microtiter plates (MTP) were performed using 96-well flat bottom black microplates. The instrument is equipped with the high energy xenon flash lamp. The instrumental parameters of the MTP reader were as follows: excitation filter of 340± 10 nm and emission filter of 614±10 nm, lag time 30 μs, integration time 100 μs, 10 flashes per well, time gap between move and flash 100 ms. Luminescence top measurement mode was used and temperature was adjusted to 25 °C.

Emission and spectral measurements of the interaction of the Eu(III)-TNB with nucleosides were carried out using A JASCO-FP6300 spectrofluorometer with 1 cm quartz cell.

UV-absorption spectra were recorded with a Shimadzu-UV Probe Version 2.33 UV-Visible automatic recording spectrophotometer with 1 cm quartz cell.

The value of the EMF of the cell was taken with a commercial Fisher Accumet pH/ion meter model 825 MP. The potentiometric system was connected to a glass electrode (Metrohm 1028) connected with a double junction reference electrode (Orion 9020). The temperature was controlled by circulation of water through the jacket from a VEB Model E3E ultrathermostat bath and maintained within (25.0±0.1) °C. Purified nitrogen was bubbled through the solution in order to maintain an inert atmosphere. Efficient stirring of the solution was achieved with a magnetic stirrer. All solutions were prepared in a constant ionic medium, 0.1 mol. dm^{-3} KNO_3. The concentration of hydrogen ion was decreased by the addition of potassium hydroxide, prepared in the ionic medium used for the solution.

The value for the K_w of water in the 5% ethanol-water mixture has been taken from the literature [51].

Gran's method [52] was used to determine $E^{o\prime}$ and E_j so that the hydrogen ion concentration, h, could be found from E, the measured potential by means of

$$E(mV) = E^{o\prime} - 59.157 \log h + E_j \quad (1)$$

Values of the ionic product of the different hydroorganic media were refined using the MAGEC program [53]. The protonation constants were then determined by use of the Bjerrum function [54].

$$n = (H_T - h + K_W/h)/A_T$$
$$= (\beta_1 h + 2\beta_2 h^2)/(1 + \beta_1 h + \beta_2 h^2) \quad (2)$$

which is calculated from the experimental quantities, h, the total concentration of titratable hydrogen ion H_T and the total reagent concentration A_T. pKa values of the investigated ligands were determined in 5% ethanol-water mixture from the overall protonation constants β_1 and β_2 calculated by the linearization method of Irving and Rossotti [55].

Initial estimates of the pK_a values were refined with the ESAB2M computer program [56].

A constant ionic strength was obtained with 0.1 mol. dm^{-3} KNO_3 and the total volume was kept at 25.0 cm^3 in the 5% ethanol-water mixture solvent in all titrations.

For both ligand protonation and metal complex formation equilibria, data were collected over the largest possible pH interval, although a number of experimental points were frequently discarded for the final stability constant calculations, especially within the range where the complexation observed was insignificant.

All the initial estimates of the formation constants of the different binary and ternary complexes formed in the present investigation have been refined using HYPERQUAD computer program [57]. The calculation of the formation constants of the ternary complexes is based on the following equilibria

$Eu^{3+} + TNB \leftrightarrow Eu^{3+}(TNB)$ 1 : 1binary complex
$Eu^{3+}(TNB) + NS \leftrightarrow Eu^{3+}(TNB)(NS)$ 1 : 1 : 1ternary complex

$$K_{M(TNB)(NS)} = \frac{\left[M_p(TNB)_q(NS)_r\right]}{\left[M^p(TNB)_q\right][NS]^r} \quad (3)$$

The overall complexation reaction involving protonation is

$$pM + qTNB + rNS + SH \rightleftharpoons M_p(TNB)_q(NS)_r(H)_s$$

$$\beta_{pqrs} = \frac{M_p(TNB)_q(NS)_r(H)_s}{[M]^p[TNB]^q[NS]^r[H]^s} \quad (4)$$

In which TNB = 4,4,4 trifluoro-1-(2-naphthyl)1,3-butanedione, NS = nucleosides adenosine, guanosine, inosine and cytidine, and M = Eu (III) in 5% (v/v) ethanol-water mixture solvent. All side reactions due to metal ion hydrolysis have been included in the calculations [54].

Cyclic voltammetry (CV), square wave voltammetry (SWV), and differential pulse voltammetry (DPP) are collected using EG and G Princeton applied research, potentiostat/galvanostat model 263 with a single compartment voltammetric cell equipped with a glassy carbon (GC) working electrode (area=0.1963 cm^2) embedded in a resin, a Pt-wire counter electrode, and Ag/AgCl electrode as reference electrode.

In cyclic voltammetry the solution was purged with pure nitrogen for 120 s and then the potential was scanned at scan rate 100 mV s^{-1} from – 0.30 to – 0.90 V. For square wave voltammetry the samples were analyzed as in cyclic voltammetry, the pulse height was 25 mV, and the SW frequency was 80 Hz and the scan increment was 2.0 mV. In differential pulse voltammetry the samples were analyzed also as in

cyclic voltammetry, but at a scan rate=36.6 mV s^{-1}. The pulse height was 25 mV, the pulse width=50 s, frequency was 20 Hz and the scan increment was 2.0 mV.

Results and Discussion

UV-vis Spectra of Eu(III)-TNB at Different pH Values

The absorption spectrum of TNB solution shows an absorption band at 330 nm corresponding to π-π* transition and a band around 250 nm corresponds n-π* transition. The addition of Eu (III) to TNB solution enhances the absorbance at 330 nm revealing the binding between TNB and Eu^{3+} ions.

The absorption wavelength of Eu(III) -TNB showed obvious pH dependence as shown in (Fig. 1). The first absorption band is attributed to the enol and the second one to the keto form. Upon increasing pH, the intensity of the absorption band located at 330 nm decreased slightly while that of the peak at 250 nm increased.

Fluorescence Spectra of Eu(III)-TNB

The fluorescence of Eu (III) ion in solution is too weak to be observed , but by introducing TNB, characteristic fluorescence of Eu (III) ion is increased by the intramolecular energy transfer process. The excitation maximum of Eu (III)-4,4,4 trifluoro-1-(2-naphthyl)1,3-butanedione (TNB) complex is at 330 nm and the emission maximum of the hypersensitive $^5D_4 \rightarrow {}^7F_2$ transition is recorded at 613 nm. Other emission bands centered at 592 nm ($^5D_0 \rightarrow {}^7F_1$), and 698 nm ($^5D_0 \rightarrow {}^7F_4$) were observed. As common for lanthanide complexes the Stokes' shift is large.

Molar ratio method (Fig not shown) confirmed the usual 1:2 host/guest binding stoichiometry for the interaction of Eu(III) ions with TNB ligand.

Interaction of Eu(III)-TNB with DNA and Nucleosides

Spectral Characteristics

The shape and band maxima of absorption spectra for the different complexes formed in solution remain unchanged, and no other absorption band of the fluorophore towards longer wavelength is noticed as indicated in (Fig. 2).Enhancement of the fluorescence band of Eu(III) -TNB has been observed after addition of different nucleosides. These observations show that the Eu(III)-complex-nucleosides interaction does not change the absorption and spectral properties. Also the formation of any emission exciplex may be discarded, since no new fluorescence peak appears at longer wavelength.

UV spectra of Eu(III) -TNB in absence and presence of DNA were studied to investigate the interaction mode between the Eu(III) -TNB and DNA. The maximum UV absorption of the Eu(III) -TNB is located at 340 nm. Here the solution containing the same concentration of DNA was used as the blank solution to observe the UV spectra of the Eu(III) -TNB-DNA complex. Spectral changes were observed (Fig not shown) when DNA is added to a solution of Eu(III) -TNB. A marked hyperchromism is observed in the 330 nm band. The interaction of the Eu(III) -TNB with DNA causes hyposochromic shift of 10 nm in the near UV absorption maximum (from 340 to 330 nm), owing to the perturbation of the complexed chromophore system upon binding to DNA.

The excitation maximum of the Eu(III) -TNB-DNA complex is decreased compared to Eu(III) -TNB complex. This indicates the interaction between Eu(III) -TNB complex and nucleic acid. The luminescence spectra of Eu(III) -TNB-DNA complex are similar to Eu(III) -TNB, but the luminescence intensity is decreased by about two folds upon addition of nucleic acid.

Effect of pH and Ionic Strength

The luminescence intensity of Eu(III) -TNB complex with DNA and nucleosides is strongly dependent on pH . TNB is β-diketones with aromatic substituent exhibits keto-enol tautomerism. It is clear that the maximum luminescence intensity of the systems is reached at pH 8.5. This is in accordance with the fact that the ligand will coordinate with Eu (III) more efficiently in its enolic form. Therefore, we choose pH 8.5 (0.1 M Tris-HCl buffer) for the further investigations.

The effect of ionic strength (known to exert a large effect on most DNA probes) was studied using NaCl . The luminescence intensity of Eu(III) -TNB in the absence of DNA experiences a slight decrease with increasing ionic strength, although the change in the luminescence intensity in presence of DNA is significant. A decrease was observed with NaCl in concentrations ranging from 1×10^{-5} M to 5×10^{-5} M. The intensity decreases when the concentration of NaCl is 3×10^{-3} M as shown in (Fig. 3). The quenching constant with NaCl ($Ksv=2.34\times10^3$ M^{-1}) was less than that with DNA [58]. From this strong effect of ionic strength it can be assumed that the interaction of Eu(III) -TNB with the phosphate groups of DNA is electrostatic interactions with groove binding rather than intercalation into helix [59, 60].

Effect of Lag and Integration Time

The triplet states of lanthanide complexes have a long lifetime. If the change of the luminescence lifetime depends on analyte concentration time-resolved (gated) measurements

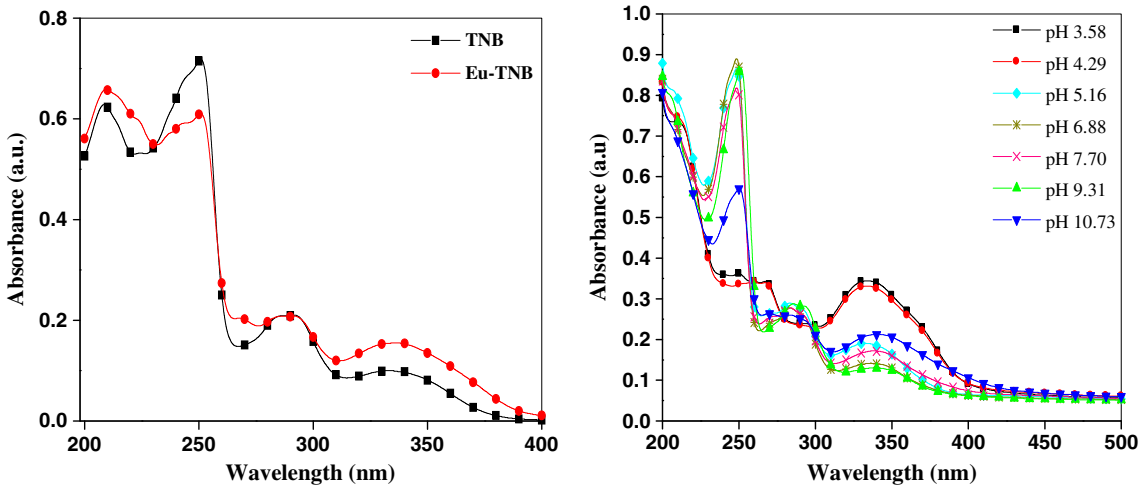

Fig. 1 Uv-vis spectra for TNB ligand and Eu(III)-complex at different pH values

can help to significantly decrease the fast-decaying background fluorescence and to obtain better sensitivity [61].The effect of different lag times on the values of F^o/F of the Eu (III) -TNB solution in the absence and presence of 10 μM nucleosides is shown in (Fig. 4). Here F^o is the fluorescence of Eu(III) -TNB in the absence of DNA and nucleosides and F is the intensity in the presence of DNA or nucleosides. Data was acquired with a 40 μs integration time. For nucleosides the ratio of F^o/F strongly decreases and then slightly increases at lag time 40 μs. For DNA data was acquired with a 40 μs integration time. The ratio of F^o/F strongly decreases until reached 40 μs and then slightly decreases at longer lag times as shown in (Fig. 5). Most of the interference from fluorescent substances is also eliminated by the use of time-resolving method.

Integration time is the length of the time period the detector exposed to emission light. (Figs. 6 and 7) show the effect of the integration time on F^o/F of Eu(III) -TNB solutions in the presence of 10 μM of nucleosides or DNA after a 40 μs lag time. If the integration time increased from 20 μs to 100 μs F^o/F decreases slowly for nucleosides . A 100 μs integration time was regarded to be appropriate. It is obvious that the integration time is not really critical.

Effect of Interferences

In order to study potential interference, samples containing 1 μmol/L of DNA, 1×10^{-5} mol/L Eu (III) and 2×10^{-5} mol/L TNB were mixed with potential interferents. Luminescence intensities were compared with a sample containing

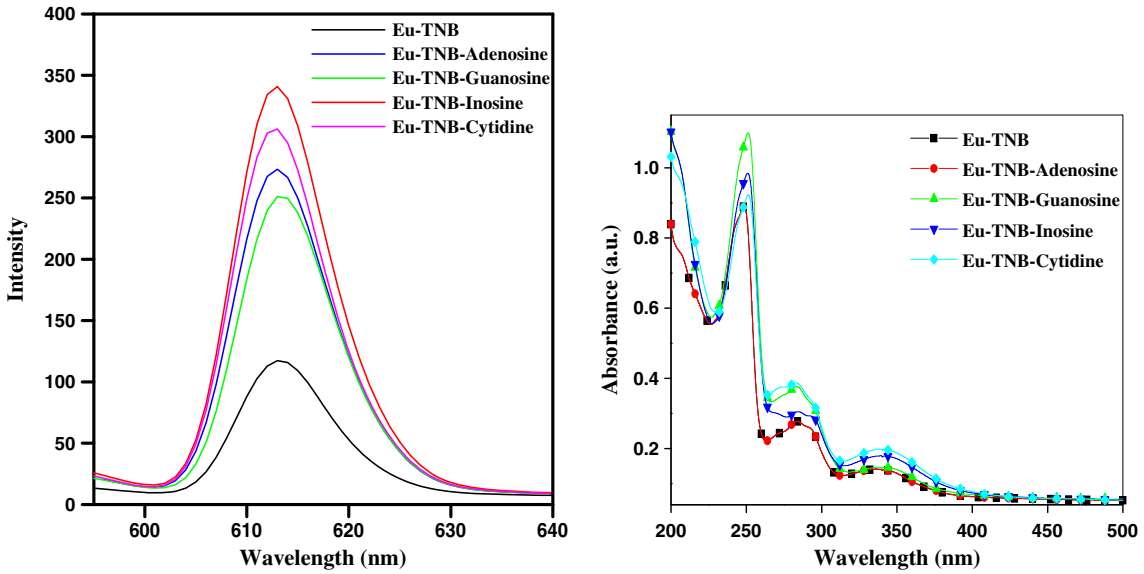

Fig. 2 UV-vis and emission spectra for Eu(III)-TNB and nucleosides under study in Tris-HCl buffer (pH 8.5)

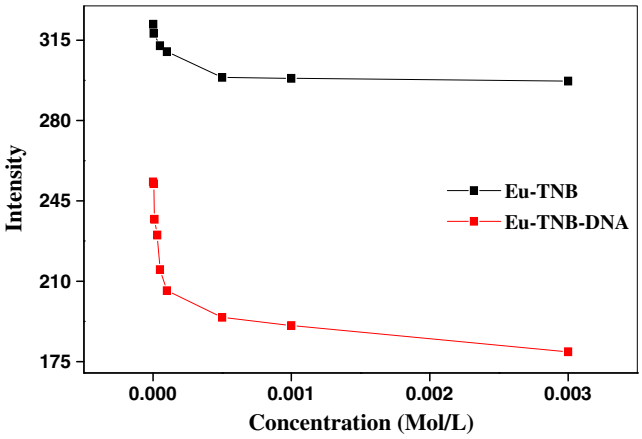

Fig. 3 Effect of ionic strength (NaCl) on the quenching luminescence intensity of Eu(III) -TNB – DNA ternary system (C_{DNA}=1 μmol/L; pH 8.5)

1 μmol/L of DNA in absence of interferent. The tolerance levels of various interferents (e.g. ions, amino acids, and saccharides) are summarized in Table 1. Most of them commonly present in biological samples are tolerated at comparatively high concentration levels. Dihydrophosphate was found to act as a quencher if present in concentration> 10 μmol/L, so phosphate is critical, in fact, phosphate buffers cannot be used.

Effect of DNA and Nucleosides on the Fluorescence Intensity of Eu(III) -TNB

The quenching of Eu(III) -TNB fluorescence intensity was studied upon addition of different concentrations of DNA in a concentration range 7×10^{-8}–7×10^{-6} M. The luminescence enhancement of the Eu(III) -TNB complex within a concentration range 7×10^{-7}–7×10^{-5} M of nucleosides was also investigated in a solution of pH 8.5 (Tris-Hcl buffer) and the data are shown in (Fig. 8). Linear calibration plots were established and given in (Figs. 9, 10 and 11). The regression data and LODs (3σ/slope) are given in Table 2.

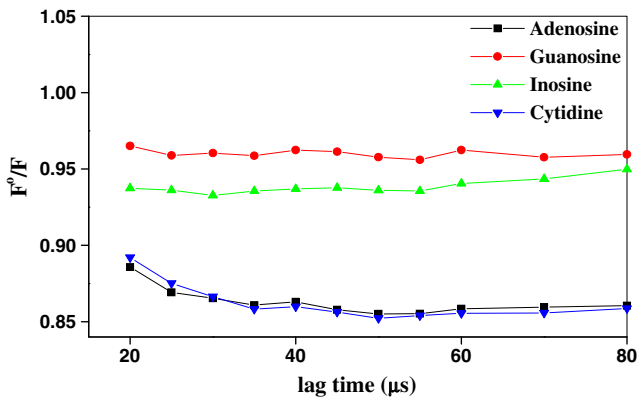

Fig. 4 Plot of F°/F versus lag time in case of nucleosides

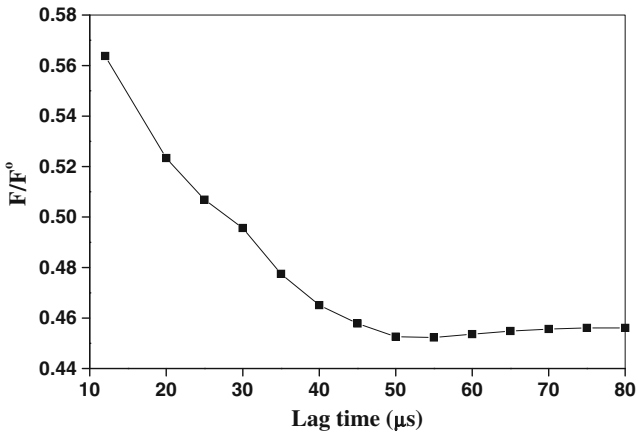

Fig. 5 Plot of F/F° versus lag time in case of DNA

To explain the europium emission enhancement of Eu (III) -TNB in the presence of nucleosides, we suggest that water molecules in the solution are grouped around the nucleoside molecules, isolating europium ions connected to TNB molecules. With less water molecules in the vicinity of europium ions, the energy transfer to water molecules is minimized, and the energy is mainly kept in the Eu ions, increasing luminescence intensity [62]. Since nucleosides are essential to life due to their important functions in biological and chemical processes , one can understand why detecting and monitoring the concentration of these species have become an attractive target for sensing/recognition studies.This approach requires, as in our case, the use of a luminescent Eu(III) complex with at least one open coordination site. This site is occupied by a solvent molecule that can be readily displaced when a nucleoside molecule is added to the solution of the coordinatively unsaturated Eu(III)-based complex. The key point is, that upon coordination of a given nucleoside to the Eu(III) ion, the structural changes in the new nucleoside-bound complex formed result in a "fingerprint" signal correlated to the added nucleoside.This will result in about two folds increase of the luminescene of Eu(III)-TNB complex after addition

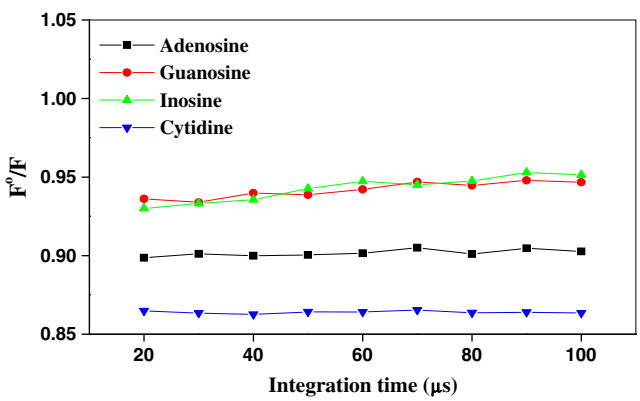

Fig. 6 Plot of F°/F versus integration time in case of nucleosides

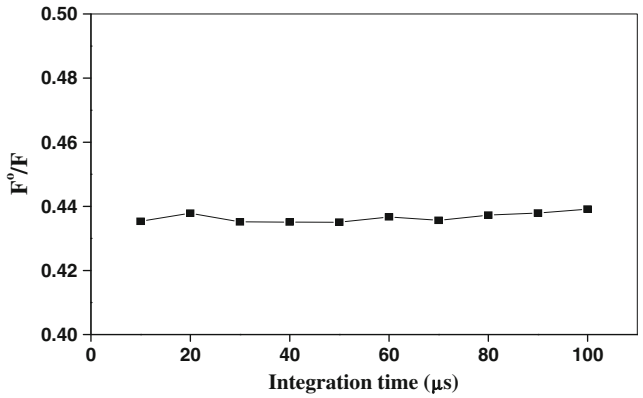

Fig. 7 Plot of F^o/F versus integration time in case of DNA

of nucleosides under investigation. So in our present study the modulation of the luminescent spectral properties of the Eu(III) -TNB probe upon the binding of a nucleoside molecule can be used for sensing/recognition purposes.

Our time-resolved mode can be used in the case of natural DNA and nucleosides samples containing many impurities, where the time-resolved detection mode might be more favorable because the background emission caused by the impurities can be effectively eliminated.

Stern-Volmer Quenching Constant

In concentration range of DNA from 7×10^{-8} to 7×10^{-6} mol/L, the fluorescence intensity of Eu(III) -TNB decreased regularly with gradual increase in the concentration of DNA. This behavior may be attributed to the possible interaction between Eu (III) -TNB and DNA . The most likely reason for such Eu(III) -TNB fluorescence quenching is due to ground state Eu(III)-TNB-DNA complex formation or collisional quenching.

The relation between DNA concentrations against the ratio F^o/F for each addition of DNA is plotted in (Fig. 12),

Table 1 Effect of conceivable interferents($C_{Eu}=1\times10^{-5}$ mol/L, $C_{TNB}=2\times10^{-5}$ mol/L and $C_{DNA}=1$ μmol/L; Tris-Hcl buffer pH 8.5)

Substance	Concentration (μmol/L)	Change of luminescence intensity
KCl	100	−2.8
$CaCl_2$	50	+8.3
NH_4Cl	50	−2.5
$Al_2(SO_4)_3$	100	+2.8
KH_2PO_4	1	+2.9
Glucose	100	−9.7
Lactose	100	−7.2
Glycine	100	−9.7
D-Alanine	50	+10.9

where F^o and F are the fluorescence intensities of Eu(III)-TNB in the absence and presence of DNA, respectively. Where the ratio F^o/F increases linearly with the DNA concentration and a linear regression equation following Stern-Volmer relation is obtained

$$F^o/F = 1 + Ksv[Q] = 1 + K_q\tau_o[Q] \quad (5)$$

One also observes that the Stern-volmer plots do not show deviation towards the y-axis (under the studied experimental concentration range) which is an indication that either static or dynamic quenching is predominant.

Temperature Dependence of Ksv

To distinguish between both static and dynamic mechanisms, their differing dependence on temperature and viscosity should be addressed. One would expect an increase of F^o/F of Eu(III)-TNB fluorescence with quencher concentration at high temperatures if collisional quenching predominates. This is because higher temperatures result in faster diffusion and hence larger amounts of collisional quenching. (Fig. 12) shows the Stern-volmer plots for quenching of Eu(III) -TNB fluorescence by the DNA at different temperatures. Also Table 3 shows that the Stern volmer quenching constant for DNA is directly proportional to temperature. The latter behavior indicates that quenching of Eu(III) -TNB by DNA is initiated by dynamic collision rather than by ground state compound formation [63]. The quenching plots illustrate that the quenching of the emission of Eu(III) -TNB is in good agreement with the linear Stern-Volmer equation.

Binding Constant at Different Temperatures

The change in the fluorescence intensity of Eu(III) -TNB in the presence of different concentrations of DNA and nucleoside was used to calculate the binding constants of Eu(III) -TNB-DNA and Eu(III) -TNB-nucleoside systems as shown in (Fig. 13). The values of the binding constants determined at different temperatures are given in Table 4 using Benesi-Hildebrand equation [64] :

$$\frac{F^\circ}{F-F^\circ} = \propto + \frac{\propto}{K[\text{Nucleoside}]},\ \propto = \frac{1}{F_L - F^\circ} \quad (6)$$

Where [nucleoside] represents the analytical concentration of nucleosides under study, F^o and F are the fluorescence intensities in the absence and presence of nucleosides, respectively, and F_L is the limiting intensity of fluorescence and α is $1/F_L$-F^o.

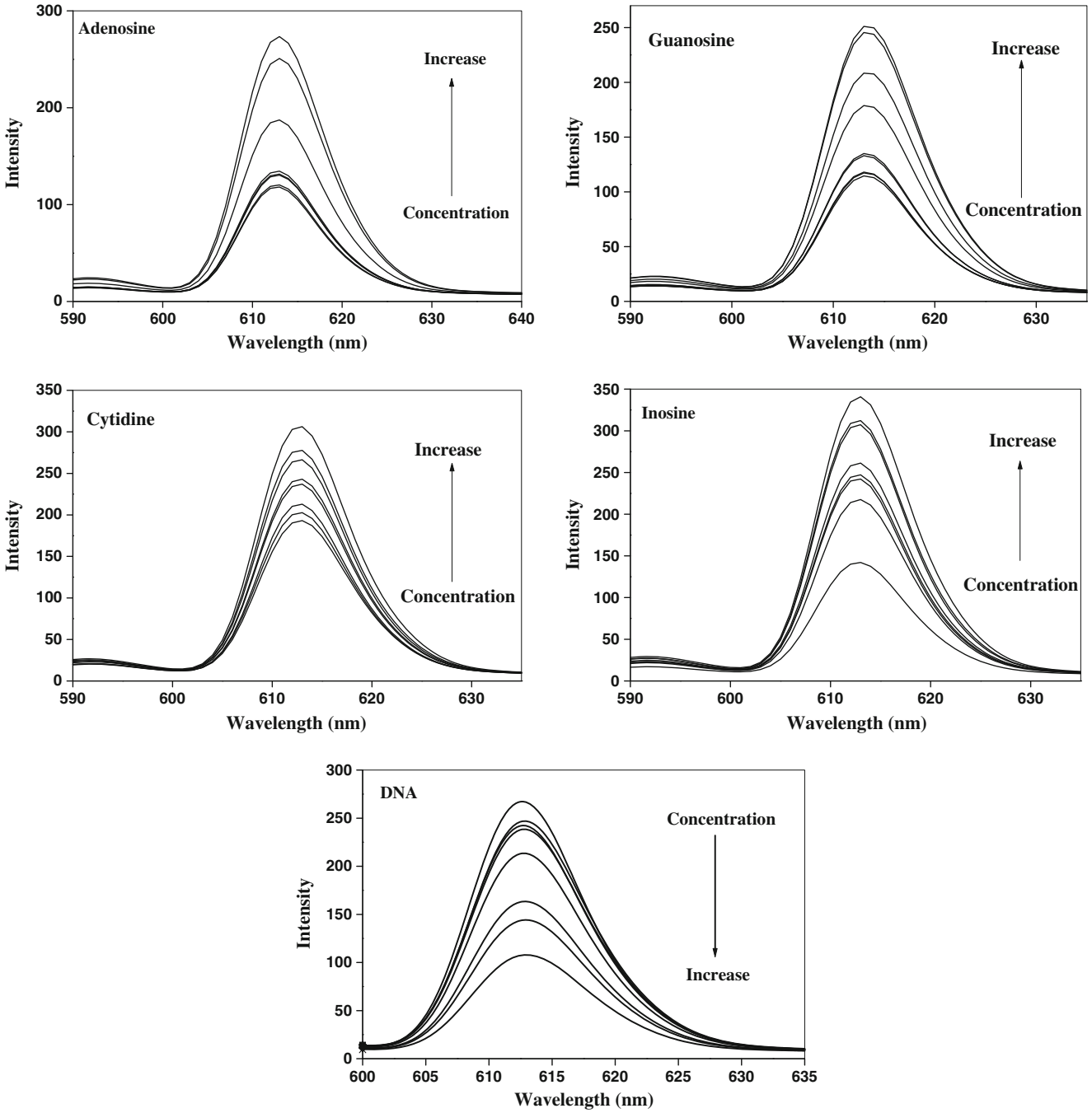

Fig. 8 Emission spectra for the ternary systems Eu(III)-TNB-DNA or nucleosides in Tris-Hcl buffer(pH 8.5)

In case of DNA the values of the binding constants determined at different temperatures are given in Table 5 using the following equation [65, 66]:

$$\mathrm{Log}\frac{F^{\circ}-F}{F} = \mathrm{LogK} + n\ \log[\mathrm{DNA}] \quad (7)$$

where K and n are the binding constant and the number of binding sites, respectively. The values of K and n are listed in Table 5. The values of n approximately equal to 1, indicating that there is one binding site in DNA for Eu(III) -TNB.

The thermodynamic parameters associated with temperature variation were analyzed in order to further characterize the acting forces between Eu(III)-TNB, DNA and nucleoside .The thermodynamic parameters, enthalpy change (ΔH) and entropy change (ΔS) of binding reaction are the main evidence for confirming binding modes. From the thermodynamic standpoint, $\Delta H>0$ and $\Delta S>0$ implies a hydrophobic interaction; $\Delta H<0$ and $\Delta S<0$ reflects the Van der Waals force or hydrogen bond formation; and $\Delta H\approx 0$ and $\Delta S>0$ suggesting an electrostatic force [67].

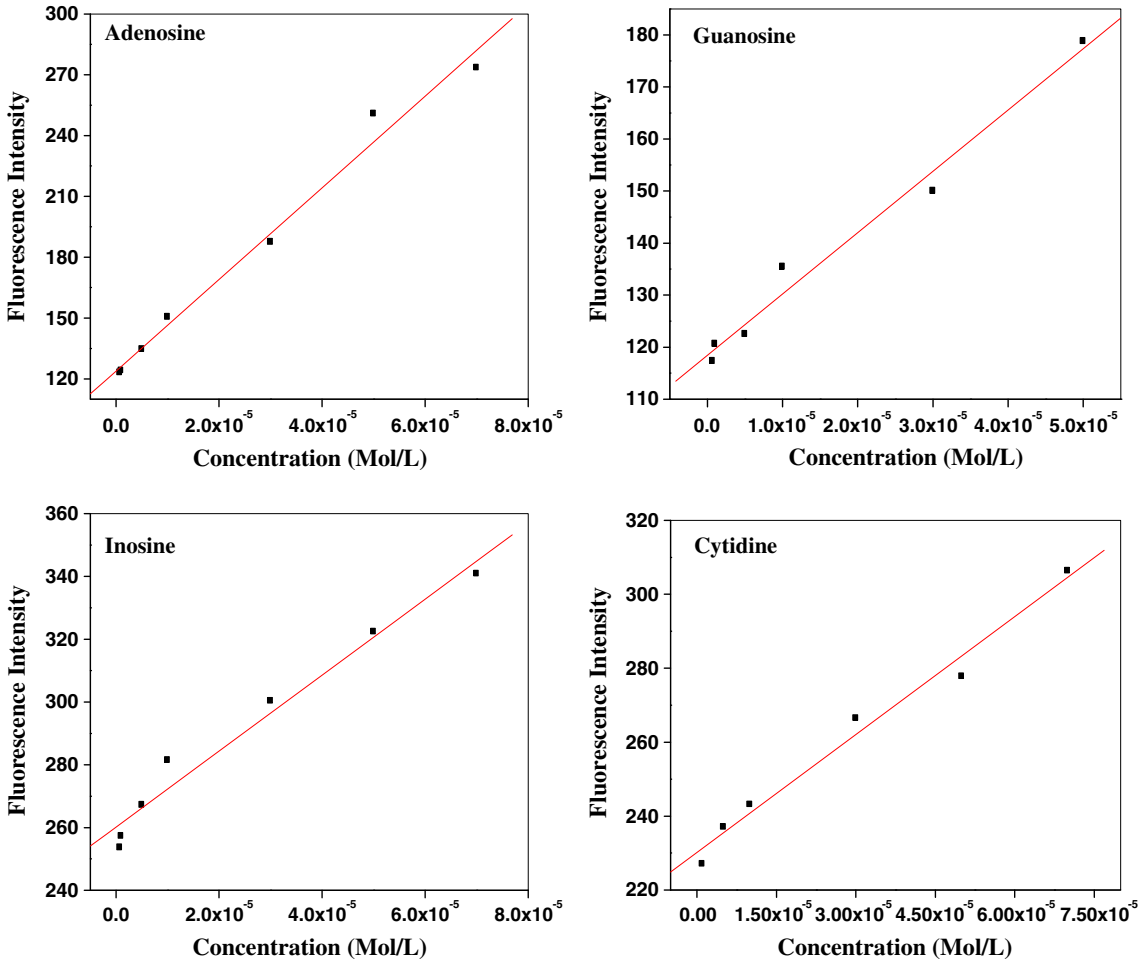

Fig. 9 Calibration plots for determination of nucleosides in Tris-Hcl buffer (pH 8.5; λ=613 nm) by normal luminescence mode

The temperature-dependence of the binding constants was studied at four different temperatures (293, 298, 303, 308, and 313 K) using the following thermodynamic equations:

$$\ln K = \Delta H/RT + \Delta S/R \tag{8}$$

$$\Delta G^\circ = \Delta H^\circ - T\Delta S^\circ = -RT \ln K \tag{9}$$

where K is the binding constant at corresponding temperature and R is the gas constant, ΔH and ΔS of reaction were determined from the linear relationship between lnK and the reciprocal absolute temperature. The free energy (ΔG^o) was calculated by Eq. (9).

Results from the plots of lnk versus 1/T (Fig. 14) are given in Table 4. The reaction of Eu(III)-TNB with DNA and nucleosides is spontaneous as indicated from the negative value for ΔG^o, both ΔH^o and ΔS^o are negative in case of adenosine and guanosine. This attributed to Van der Waals force or hydrogen bond formation. The large value for the entropy change also suggests that the binding process is mostly entropy driven. In case of inosine and cytidine ΔH^o has a very small negative value, while ΔS^o has a positive value, suggesting an electrostatic interactions. In case of DNA small positive value of ΔH^o may be attributed to electrostatic interactions being the leading contributor to the binding. A positive value for ΔS^o is also associated with electrostatic interactions and hence the metal complex interaction with DNA is controlled by electrostatic nature. The large value for the entropy change also suggests that the binding process is mostly entropy driven.

Potentiometric Measurements

Potentiometric measurements for the interaction of nucleosides adenosine, guanosine, inosine and cytidine with Eu (III) and 4,4,4 trifluoro-1-(2-naphthyl)1,3-butanedione (TNB) have been carried out .

The formation of the binary Eu(III)-nucleosides (NS), and Eu(III)-TNB in 1:1 ratio in addition to Eu(III) -TNB-NS 1:1:1 ternary complex species are inferred from the

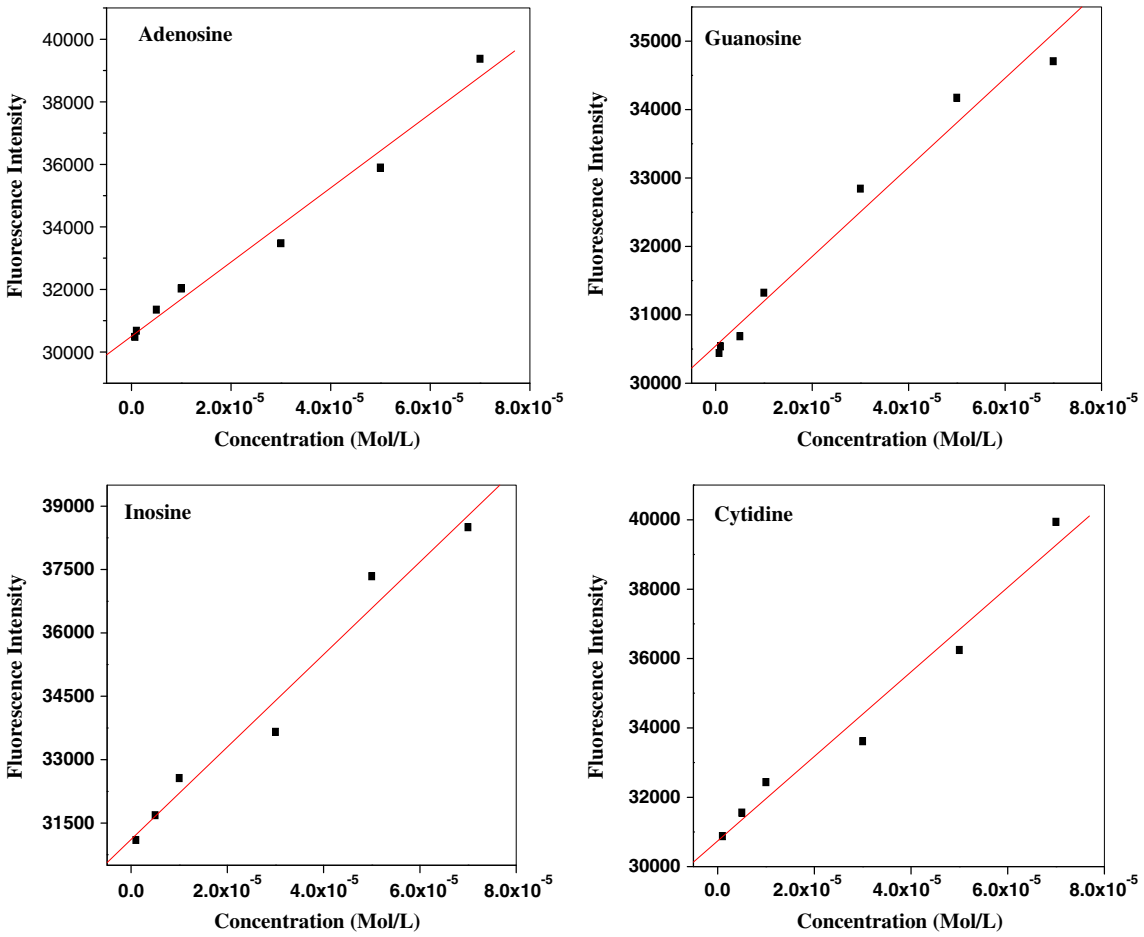

Fig. 10 Calibration plots for determination of nucleosides in Tris-Hcl buffer (pH 8.5; λ=613 nm) by time-resolved fluorescence mode

potentiometric pH titration curves. Initial estimates of the stability constants of the resulting species and the acid dissociation constants of nucleosides and 4,4,4 trifluoro-1-(2-naphthyl)1,3-butanedione (TNB) have been refined with the HYPERQUAD computer program [57]. The quality of the fit during this refinement was judged by the values of the sample standard deviations and the goodness of fit χ^2 (Pearson's Test). At σ_E=0.1 mV (0.001 pH error) and σ_V=0.005 ml, the values of S in different sets of titrations were between 1.0 and 1.7 and χ^2 was between 12.0 and 13.0. The scatter of residuals (E_{obs}-E_{calc}) versus pH reasonably random, without any significant systematic trends, thus indicating a good fit of the experimental data of the expected model systems under our experimental conditions.

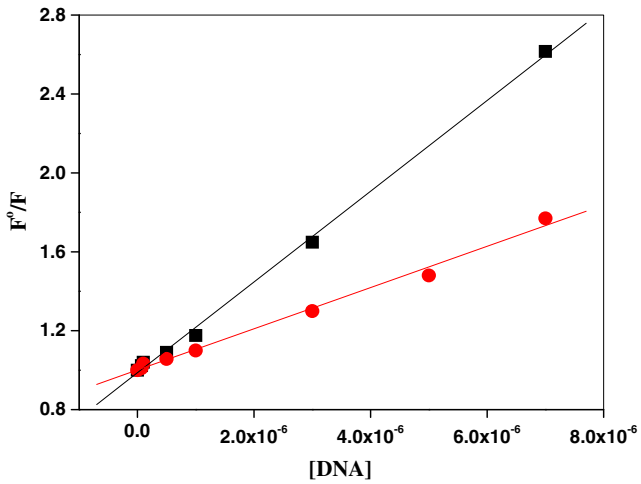

Fig. 11 Comparison of intensity-based (F^o/F) by normal luminescence mode (squares) and the time-resolved mode (circles)

Furthermore the formation constant values of the different 1:1 Eu(III)-nucleoside binary complexes have been determined under identical conditions. This is made with the aim to compare the stability of the formed 1:1:1 ternary complex with that of the corresponding 1:1 binary metal complexes.

The data collected in the pH range 3.0 – 11.0 (Figs not shown) were used for the calculations and refinements.

The formation constants of all the binary and the ternary complexes studied are given in Table 6.

The calculated dissociation constant of TNB is found to be 5.30±0.02 at I=0.1 mol.dm^{-3} KNO_3 and at 25 °C. The

Table 2 Parameters of curves calibrations obtained for the determination of DNA and nucleosides where R: correlation coefficients; s: slope of the working curves; and *DL*: detection limits at 25 °C

Nucleoside	The time-resolved mode			The normal luminescence mode		
	R	s $mol^{-1}.L$	*DL* (μmol L^{-1})	R	s $mol^{-1}.L$	*DL* (μmol L^{-1})
Adenosine	0.9910	1.19×10^{8}	6.30	0.9932	2.26×10^{6}	5.47
Guanosine	0.9873	6.52×10^{7}	7.49	0.9907	1.18×10^{6}	4.99
Inosine	0.9858	1.09×10^{8}	9.59	0.9858	1.21×10^{8}	7.94
Cytidine	0.9856	1.22×10^{8}	9.63	0.9911	1.06×10^{6}	7.54
DNA	0.9963	1.05×10^{5}	0.74	0.999	2.03×10^{5}	0.38

formation constant of Eu (III)-TNB binary complex is calculated and refined through HYPERQUAD computer program and is found to be 5.28±0.02.

To the author's knowledge no data for the ternary complexes containing TNB with the nucleosides guanosine, adenosine, inosine, and cytidine are available in the literature for comparison.

In our study we have three purine nucleosides adenosine, guanosine, inosine and one pyrimidine nucleosides cytidine. There are few examples of structure determination of metal complexes of nucleosides, as compared to those of nucleotides and of the purine and pyrimidine bases. In the structure of metal-purine complexes it has been found that the predominant mode of metal binding takes place at the nitrogen atoms of the five-membered (imidazole) ring N7 and N9 and also (in some adenine complexes) at the N3 and N1 positions of the six-membered (pyrimidine) ring. For purine nucleosides, however, the presence of the sugar ring reduces the number of coordination sites available. N9 is, of course blocked, and the N3 position, which is not a strong ligating position. This leaves N7 and O6 of guanine and N7 and N1 of adenine as possible metal-binding sites[68, 69].

Metal complexes of pyrimidine nucleosides have been studied less extensively than those of purine nucleosides. This may be partly due to the fact that the pyrimidine nitrogen N3 is a weaker ligating atom than the imidazole nitrogen N7 of purines. Generally there is direct involvement of nucleobase moiety in the metal coordination sphere in the metal nucleosides complexes.

In the purine nucleosides binding may occur at N1 or N7. The former nitrogen is protonated in neutral solutions of inosine (pK_a=8.8) and guanosine (pK_a=9.2), so that a metal ion may coordinate the weakly basic N7 or compete with the proton for the more basic N1. For weakly basic adenosine with pK_a 3.6 for N1, in neutral solutions both the N1 and N7 sites are free to bind metal ions [68, 69]. The dissociation constant values for the nucleosides were estimated to be for adenosine (pK_a N1=3.60±0.02), cytidine (pK_a N3=4.20±0.02), guanosine (pK_{a1} N7=2.10±0.02, pK_{a2} N1=9.20±0.03) and inosine (pK_{a2} N1=9.20±0.02).The obtained values are in good agreement with literature[69].

During our refinements the data fit well with the model protonated ternary system in the input instruction of the HYPERQUAD calculation indicating the possibility of the formation of monoprotonated ternary systems of the type Eu (III)(TNB)(HNS) in solution. For the ternary complexes formed in solution the refined stability constant values follows the order: guanosine>inosine>cytidine>adenosine.

The higher values for the stability constants of ternary complexes compared with those of the binary systems as given by the values of $\Delta\log K_M$ shown in Table 6 may be attributed to the interligand interactions or some cooperatively between the coordinated ligands, possibly H-bond formation. This also may be explained on the basis of the π-electron donating tending of the Eu (III) ion to the antibonding π* orbital of the heteroaromatic N base, strengthens of the Eu (III)-N bond. Due to the back donation from metal to base, the f-electron density on the metal decreases,

Table 3 The Stern-Volmer constants (Ksv) of Eu(III)-TNB-DNA ternary system at different temperatures

Temperature	Ksv (M^{-1})	R
293 K	1.82×10^{5}	0.999
298 K	2.03×10^{5}	0.999
303 K	2.30×10^{5}	0.998
308 K	2.64×10^{5}	0.997
313 K	3.10×10^{5}	0.995

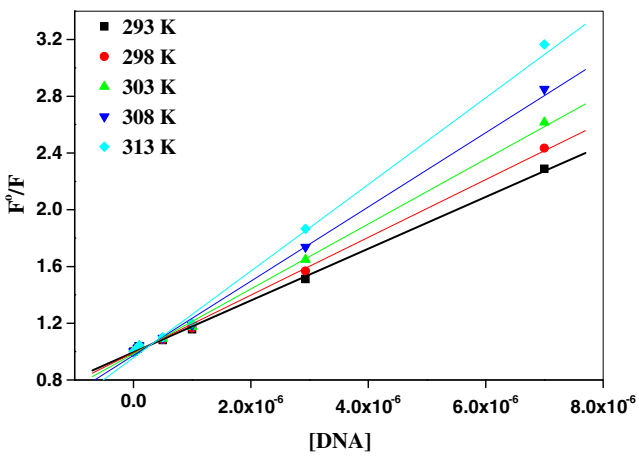

Fig. 12 Intensity-based (F^o/F) Stern-Volmer plots for DNA at different temperatures

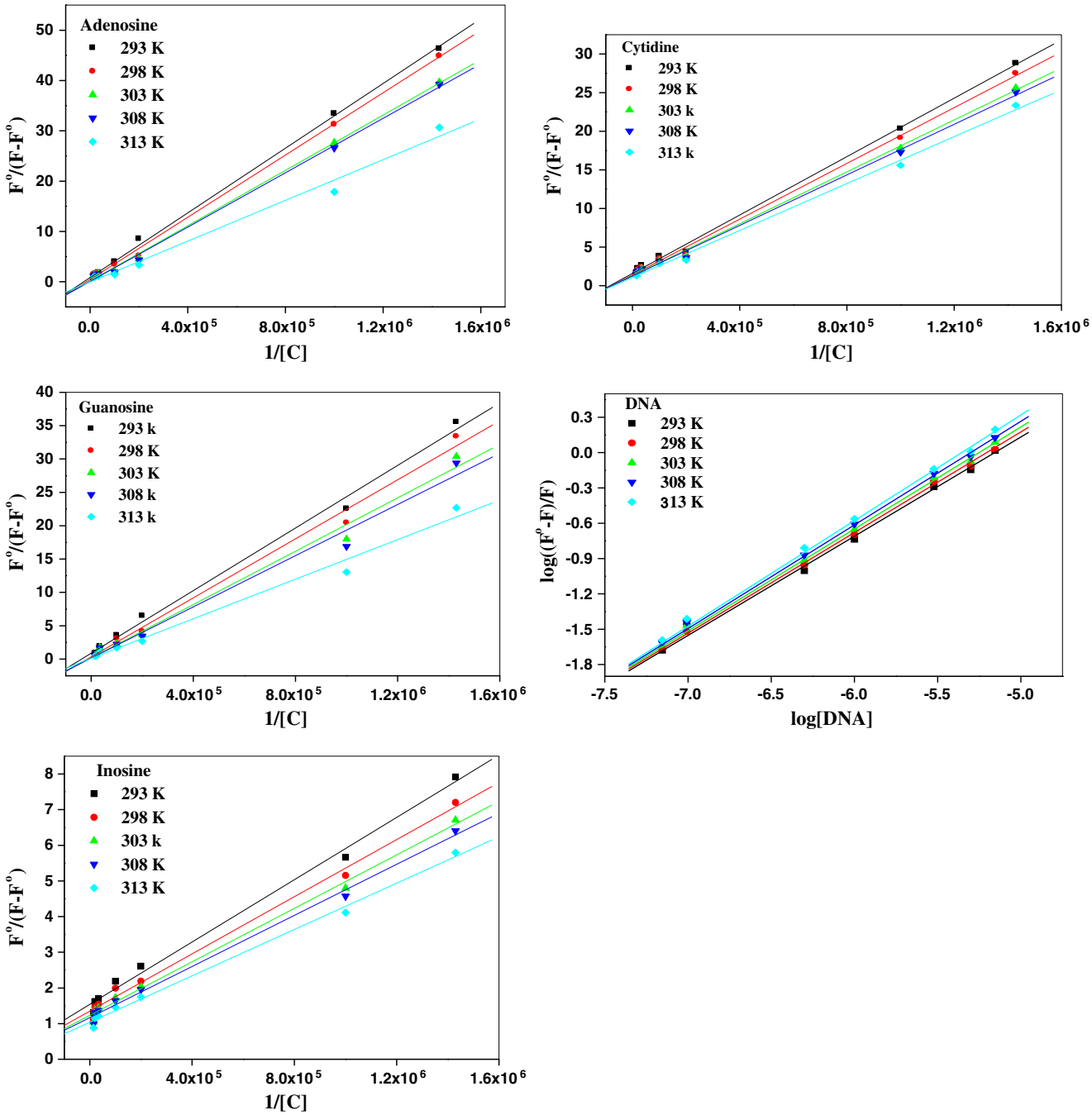

Fig. 13 The binding curves for the ternary systems Eu(III)-TNB-DNA or nucleosides at different temperatures

this renders the metal more electrophilic. The interaction of the π-electrons of the secondary ligands with the metal will increase to a greater extent and consequently enhance the formation of the mixed ligand complexes.

The behavior described above, is better observed in the distribution species diagrams as a function of pH of these systems (Fig. 15(a–d)). Based on our potentiometric studies the proposed chemical structures for the binary and ternary complexes are given in Scheme 2.

Electrochemical Studies of the Interaction of Eu(III) -TNB with Nucleosides and DNA

Representative cyclic voltammograms for the binary and ternary systems including Eu(III),TNB,nucleoside or DNA are shown in (Figs. 16, 17, 18 and 19) . It is clearly observed that the reduction process of Eu(III) metal ions proceeds via quasi –reversible electrochemical process at the glassy carbon electrodes involving one electron transfer step

Table 4 Binding constants and thermodynamic parameters for the interaction of Eu(III)-TNB with the nucleosides under study

	Temp	Binding constant K($Lmol^{-1}$)	R	ΔH (kJ/mol)	ΔS (J/mol.k)	ΔG° (kJ/mol)
Adenosine	293 K	2.63×10^4	0.9994	−144.18	−405.81	−24.80
	298 K	1.46×10^4	0.9992			−23.76
	303 K	4.91×10^4	0.9989			−21.41
	308 K	1.85×10^3	0.9987			−19.26
	313 K	6.52×10^2	0.9986			−16.86
Guanosine	293 K	3.80×10^4	0.9974	−56.03	−106.17	−25.70
	298 K	1.54×10^4	0.9964			−23.88
	303 K	9.70×10^3	0.9947			−23.13
	308 K	8.45×10^3	0.9929			−23.15
	313 K	8.31×10^3	0.9929			−23.50
Inosine	293 K	3.53×10^5	0.9968	−3.52	94.11	−31.11
	298 K	3.38×10^5	0.9968			−31.54
	303 K	3.29×10^5	0.9977			−31.99
	308 K	3.27×10^5	0.9976			−32.52
	313 K	3.19×10^5	0.9975			−32.97
Cytidine	293 K	8.35×10^4	0.9990	−4.87	77.49	−27.60
	298 K	7.81×10^4	0.9988			−27.92
	303 K	7.74×10^4	0.9988			−28.37
	308 K	7.68×10^4	0.9987			−28.81
	313 K	7.15×10^4	0.9980			−29.09

based on the electrichemical analysis of the given cyclic votammograms.

The complexation of Eu (III) with TNB is accompanied by a shift in the reduction potential to more negative value, and decrease in the cathodic peak current i_{pc} which may be attributed to complexation with TNB.

Due to the presence of more electrons withdrawing CF_3 group, the electron density on the metal center is reduced considerably, this results in higher redox potential [70–72].

On increasing the scan rate from 25 to 100 mVs^{-1} in the cyclic voltammograms for Eu(III)-TNB binary complex, both cathodic and anodic peaks are shifted to more negative and positive potential, respectively confirming the irreversible nature of the observed redox process [73].

The cathodic reduction potential for the interaction of Eu (III) -TNB binary complex with nucleosides under study is shifted to less negative value with respect to Eu(III) -TNB curve by 82, 24, 12 and 7 mV for guanosine, cytidine, inosine and adenosine, respectively which may be attributed to the high degree of binding with guanosine. This possible selectivity towards guanosine nucleoside will be very interesting in the current research in our lab concerning drug discovery based on our new lanthanide compounds. Discovery of novel sensors for guanosine based on the luminescent Eu(III)-TNB probe is now under investigation in our lab.

The reaction of the Eu(III) -TNB with DNA molecules reflects itself through the reduction peak shifted to less negative value by 8 mV, and reduces in cathodic current by 1.94 μA.

The oxidation of Calf-thymus DNA on the surface of the glassy carbon electrode was studied in 0.1 M phosphate buffer at 25 °C, where two oxidation peaks are observed at + 0.72 and + 1.02 V in the cyclic voltammogram. The two anodic peaks are attributed to the oxidation of guanine and adenine bases. The obtained results are in good agreement with the values found in literature [74]. The oxidation peak located at 0.72 V disappears which indicate the interaction of Eu(III) -TNB with guanine moiety.

The complexation of Eu (III) with TNB is confirmed using differential pulse technique. The reduction peak of Eu(III) –TNB is shifted to more negative value by −78 mV with a decrease in cathodic current by 0.79 μA which may attributed to strong interaction of Eu (III) with TNB as shown in (Fig. 20).

The effect of scan rate was studied in the range of 5–36 mV/s. Eu(III) -TNB complex exhibits an increase in the reduction current with an observable shift to more negative value.

The interaction of Eu (III)-TNB binary complex with nucleosides is shown in (Fig. 21). A considerable shift to the less negative value with respect to Eu (III) -TNB curve by 34, 18, 28, and 18 mV were observed for guanosine, cytidine, inosine and adenosine ,respectively, which may be

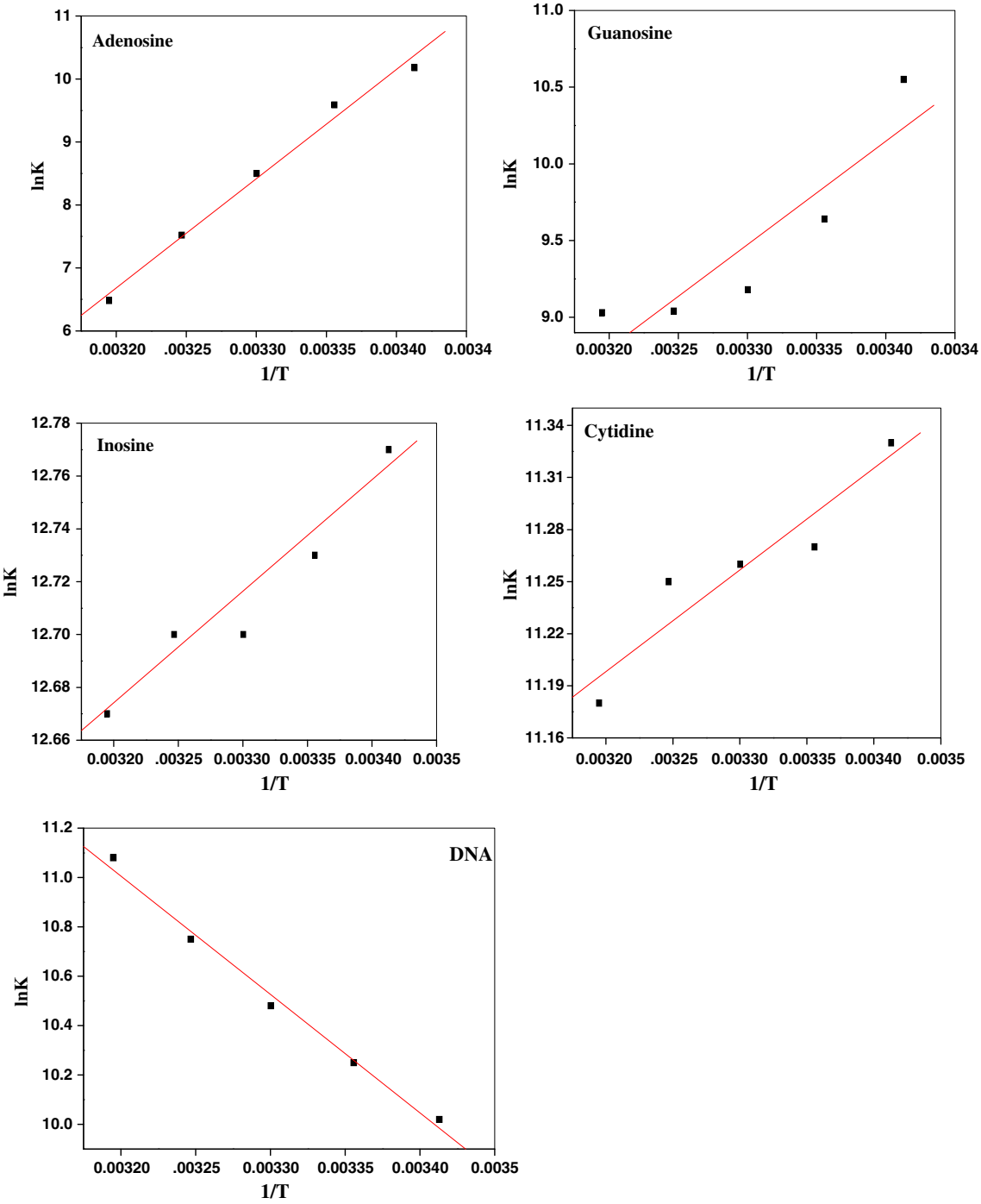

Fig. 14 Correlation between Ln k versus 1/T for the ternary systems under investigation

Table 5 Binding constants, n and thermodynamic parameters for the interaction of Eu(III)-TNB with DNA

Temp.	Binding constant logK ($Lmol^{-1}$)	n	R	H Δ(kJ/mol)	S Δ(J/mol.k)	G°Δ (kJ/mol)
293 K	4.35	0.84	0.991	3.88	219.16	−24.41
298 K	4.45	0.85	0.990			−25.40
303 K	4.55	0.87	0.989			−26.40
308 K	4.67	0.88	0.988			−27.53
313 K	4.81	0.90	0.987			−28.83

Table 6 Formation constants for the Eu(III) -nucleosides and Eu(III)-TNB binary complexes and those for the mixed ligand complexes Eu(III)-nucleoside-TNB at (25.0±0.1) °C in 5% (v/v) ethanol -water mixture and ionic strength I=0.1 mol.dm^{-3} KNO_3

Ligand	^{logK}Eu (III) (NS) or ^{logK}Eu (III) (TNB)	^{logK}Eu(III)(TNB)(NS)	$\Delta logK_M$
Guanosine	4.27±0.02	17.96[b]±0.03	–
Adenosine	4.30±0.02	4.34[a]±0.02	+ 0.04
Inosine	4.30±0.02	8.69[a]±0.02	+ 4.39
Cytidine	4.31±0.01	5.07[a]±0.03	+ 0.76
TNB	5.28±0.03		

±refers to three times standard deviation (3σ)

[a] log formation constants of normal ternary complex log $K_{Eu(III)(TNB)(NS)}$

[b] log formation constants of protonated ternary complex log $K_{Eu(III)(TNB)(HNS)}$ $\Delta \log K_M = \log K_{Eu(III)(TNB)(NS)} - \log K_{Eu(III)(NS)}$

attributed to the high degree of binding with guanosine. The favorable reduction potential of the ternary system including guanosine may be attributed to the presence of adsorption character of this ternary system at the surface of the glassy carbon electrode. This behavior agrees well with the experimental data obtained from cyclic voltammetry.

The reaction of the Eu(III) -TNB with DNA molecules is confirmed by differential pulse polarograms. The reduction peak of Eu(III) -TNB at 716 mV shifted to less negative value by 14 mV, with decreasing in cathodic current as shown in (Fig. 22) indicating a considerable interaction between the complex and DNA.

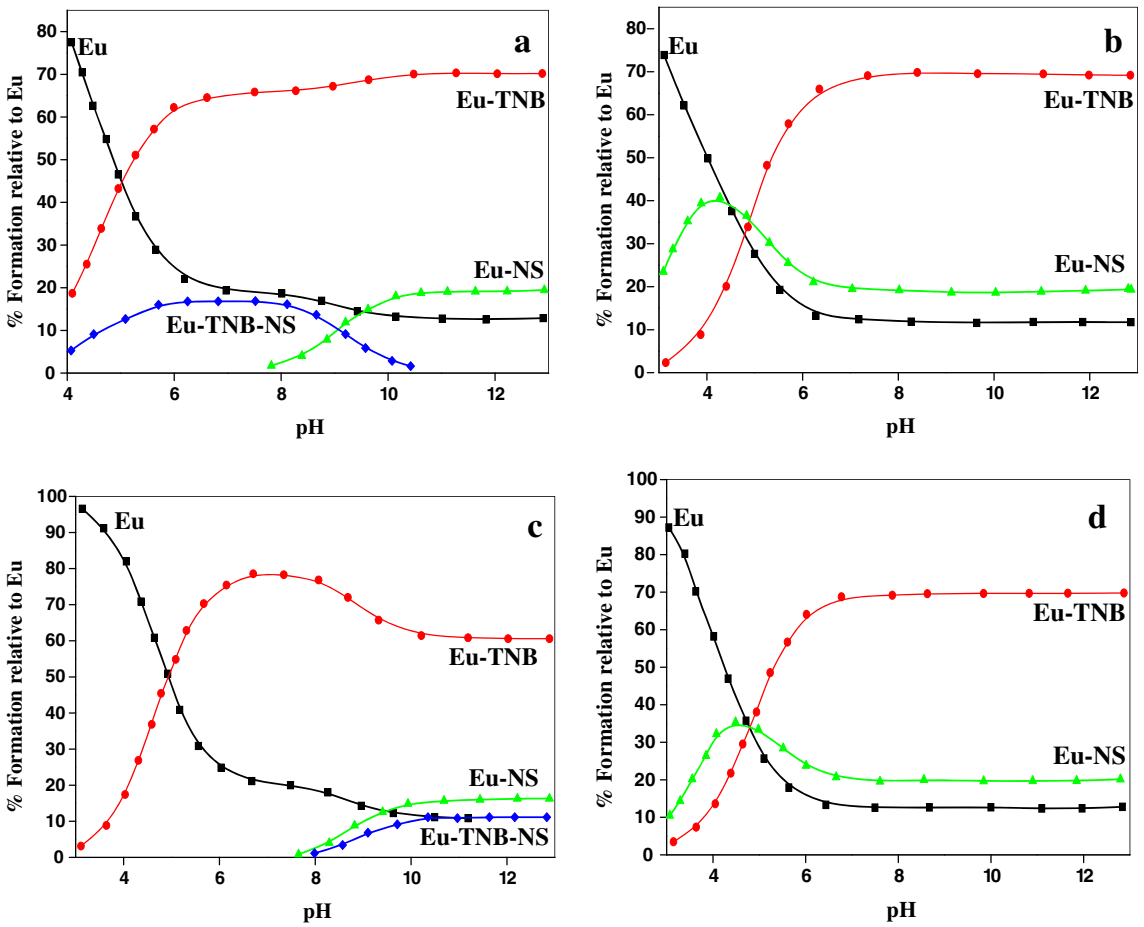

Fig. 15 Distribution diagrams as a function of pH for the system Eu(III)-TNB-NS in the ratio 1:1:1 at 25 °C and I=0.1 mol.dm^{-3} KNO_3. NS = (**a**) guanosine, (**b**) adenosine, (**c**) inosine, and (**d**) cytidine

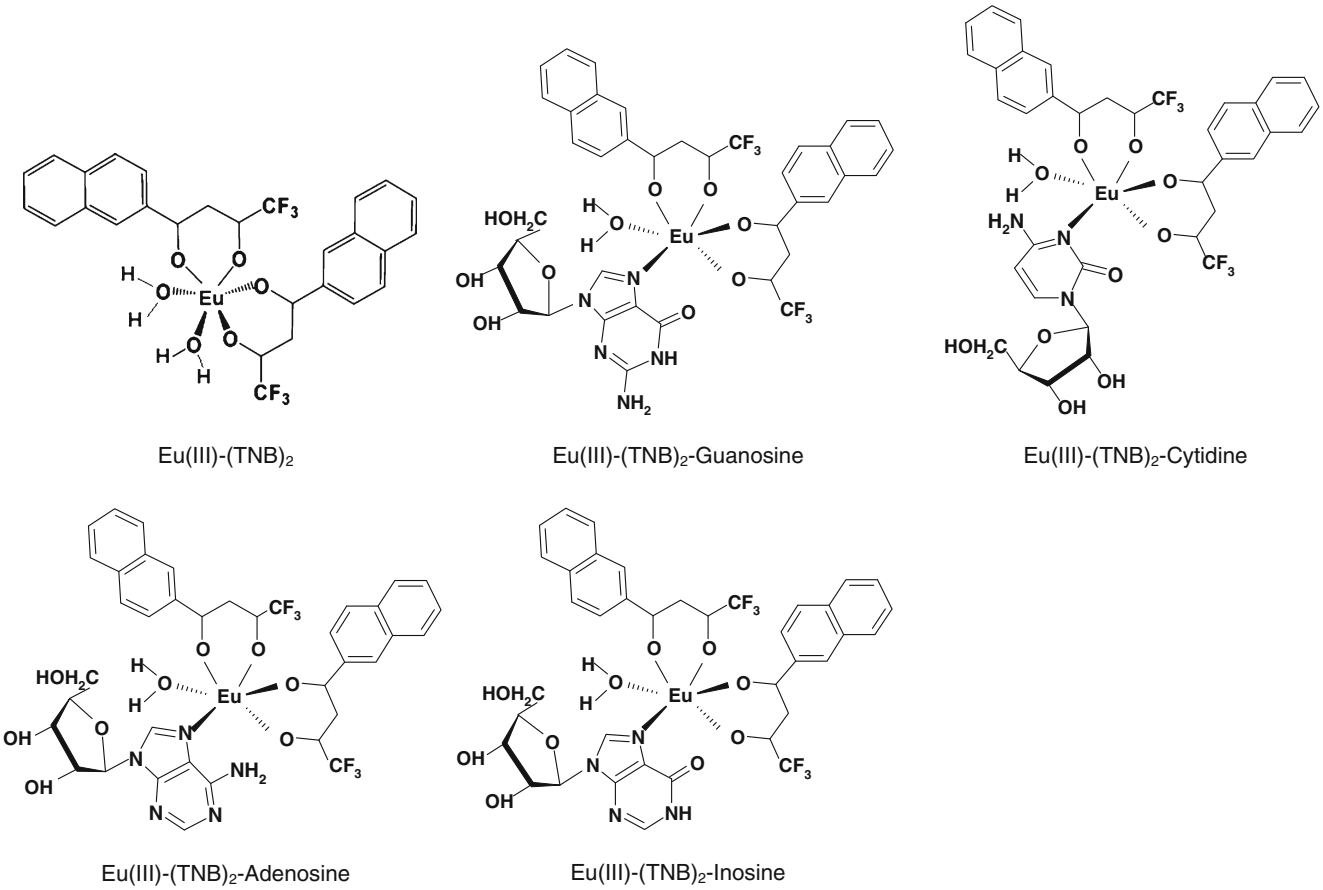

Scheme 2 Proposed chemical structures for the binary and ternary complexes of the systems under investigation

The differential pulse polarogram (DPP) for DNA oxidation on the surface of glassy carbon electrode also displays a two well defined oxidation peaks at + 0.69 and at + 0.96 V which may be attributed to the characteristics anodic peaks of guanine and adenine bases in DNA molecule.

The interaction of Eu(III) -TNB with DNA molecules will perturb the two peaks, where the oxidation peak of guanine is splitted into two oxidation peaks at 0.77 and at 0.67 V. This behavior confirms the selectivity of Eu(III)-TNB towards guanine moiety. The complexation behavior

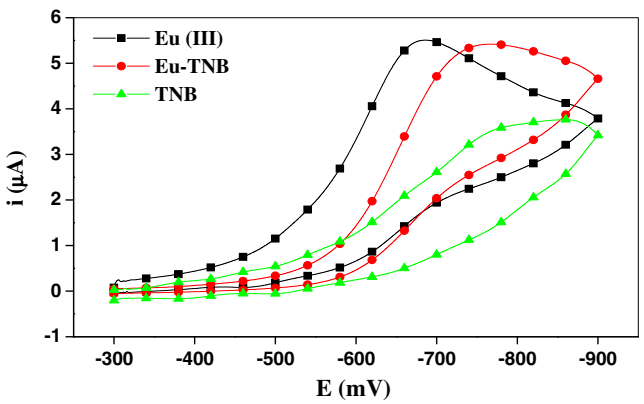

Fig. 16 Cyclic voltammograms for the binary system Eu(III)-TNB in 0.1 M p-toluenesulfonate, scan rate=50 mV/s and at 25.0 °C [$C_{Eu}=1\times10^{-4}$ M, $C_{TNB}=2\times10^{-4}$ M]

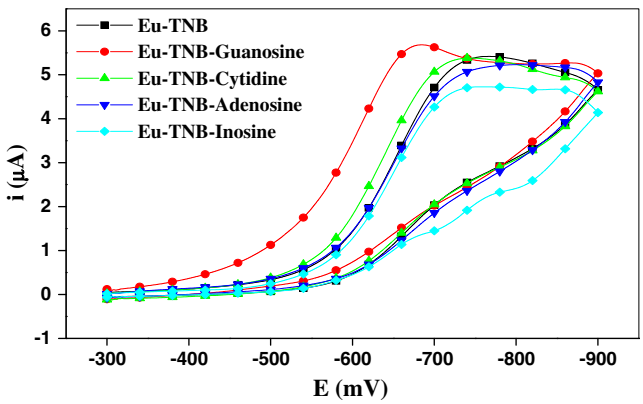

Fig. 17 Cyclic voltammograms for the ternary systems of the type Eu (III)-TNB-nucleoside in 0.1 M p-toluenesulfonate, scan rate=50 mV/s and at 25.0 °C [$C_{Eu}=C_{Nucleosides}=1\times10^{-4}$ M, $C_{TNB}=2\times10^{-4}$ M]

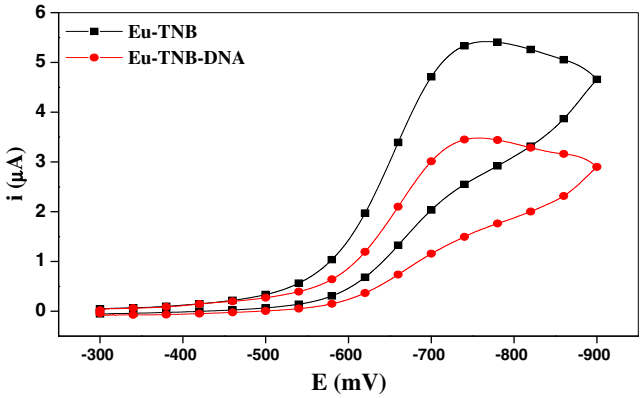

Fig. 18 Cyclic voltammograms for the ternary system Eu(III) -TNB-DNA in Tris-Hcl buffer(pH=8.5), I=0.1 M p-toluenesulfonate, scan rate=50 mV/s and at 25 °C. [$C_{Eu}=1\times10^{-4}$ M, $C_{TNB}=2\times10^{-4}$ M, and $C_{DNA}=1\times10^{-5}$ M]

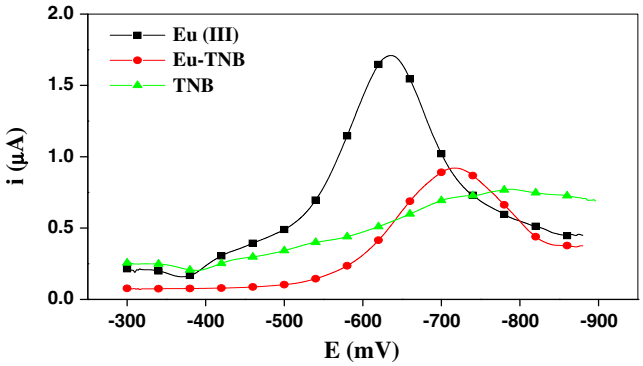

Fig. 20 Differential pulse polarograms for the binary system Eu(III)-TNB in 0.1 M p-toluenesulfonate, scan rate=25 mV/s and at 25.0 °C. [$C_{Eu}=1\times10^{-4}$ M, $C_{TNB}=2\times10^{-4}$ M]

of Eu (III) with TNB is further confirmed using square wave voltammetric technique. The reduction peak of Eu(III)-TNB is shifted to more negative value with decreasing in cathodic current indicating a strong interaction of Eu (III) with TNB as shown in (Fig. 23).Selectivity of our novel Eu(III)-TNB towards guanine base during our studies may has interesting biological applications in the field of drug discovery. G-quadruplexes are highly stable alternative DNA structures formed by tetrads of guanines that interact via Hoogsteen hydrogen bonds and are stabilized by monovalent cations [75–78]. A number of conformationally diverse G-quadruplex structures have been determined by NMR or X-ray crystallography [79–82]. G-quadruplexes have been shown to occur at telomeres [83, 84], and have potential as a target class for therapeutics [85–87].Biomedical applications and the possibility of using our novel Eu(III) -TNB complex as anticancer drug is currently under investigation in our lab. Many natural and synthetic anticancer agents with the ability to interact with DNA have been discovered, but most have little sequence-specificity and often exhibit severe toxicity to normal tissues. Thus, there has been considerable interest in molecular biology and human medicine to find small molecules that can bind the DNA in a sequence-specific manner and modify the function of nucleic acids irreversibly. Analogs of naturally occurring antitumor agents, such as distamycin A, which bind in the minor groove of DNA, represent a new class of anticancer compounds currently under investigation. Distamycin A has driven researchers' attention not only for its biological activity, but also for its nonintercalative binding to the minor groove of double-stranded B-DNA, where it forms a strong reversible complex preferentially at the nucleotide sequences consisting of 4–5 adjacent adenine-thymine (AT) base pairs[88]. The luminescent Eu(III)-TNB complex under investigation has affinity to DNA to bind to the minor groove and not to intercalate .This behavior may be attributed to the high electonegativity of the CF_3 group in the probe which owes its DNA-interactive and

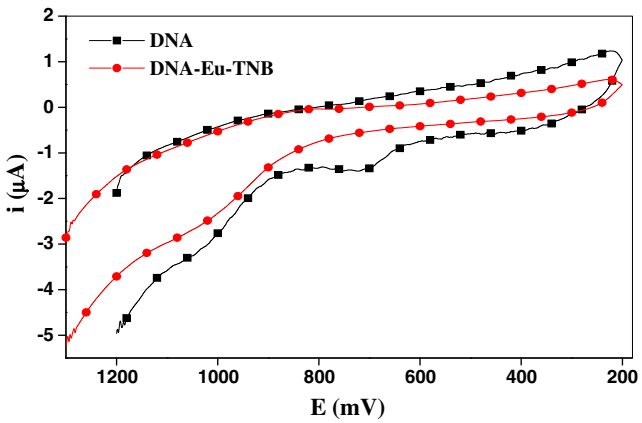

Fig. 19 Cyclic voltammograms for the ternary system DNA-Eu(III)-TNB in 0.1 M phosphate buffer pH 7.0, scan rate=100 mV/s and at 25.0 °C. [$C_{Eu}=1\times10^{-4}$ M, $C_{TNB}=C_{DNA}=2\times10^{-4}$ M]

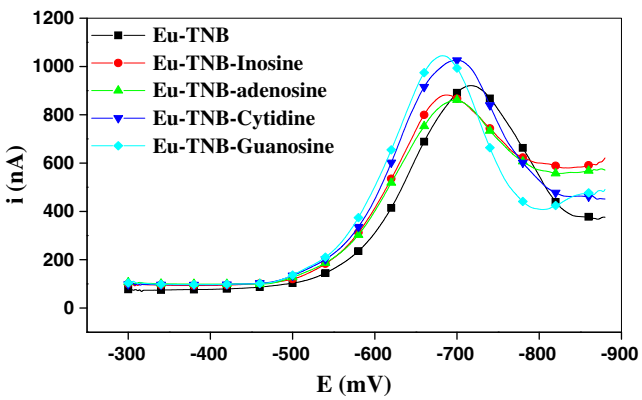

Fig. 21 Differential pulse polarograms for the ternary systems of the type Eu(III) -TNB-nucleoside in 0.1 M p-toluenesulfonate, scan rate= 25 mV/s [$C_{Eu}=C_{Nucleosides}=1\times10^{-4}$ M, $C_{TNB}=2\times10^{-4}$ M]

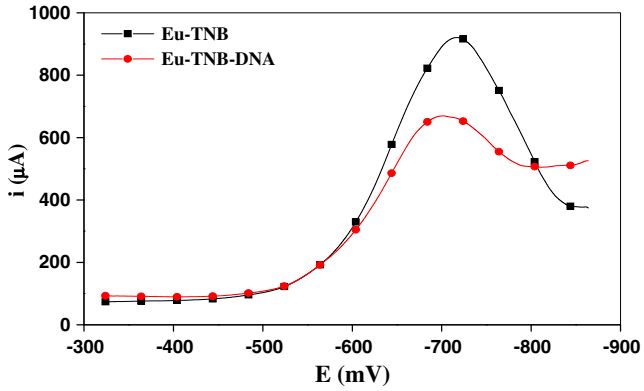

Fig. 22 Differential pulse polarograms for the ternary system Eu(III)-TNB-DNA in 0.1 M p-toluenesulfonate, scan rate=25 mV/s and at 25.0 °C [$C_{Eu}=1\times10^{-4}$ M, $C_{TNB}=2\times10^{-4}$ M, and $C_{DNA}=1\times10^{-5}$ M]

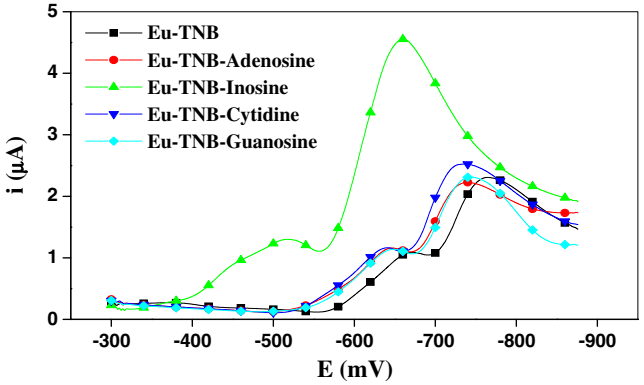

Fig. 24 Square wave voltammograms for the ternary systems of the type Eu(III)-TNB-nucleoside in 0.1 M p-toluenesulfonate, frequency=20 Hz, and at 25.0 °C

is capable of covalently binding to the C_2-NH_2 of guanine residues in the minor groove of DNA.

Eu (III)-TNB exhibits two reduction peaks, the first one shifted to less negative values by 20, 104, 26 and 28 mV by addition of guanosine, inosine, adenosine and cytidine, respectively as indicated in (Fig. 24).

The peak located at 764 mV is shifted to less negative values by 6 mV after addition of DNA and current decreases by 0.66 μA which indicates the binding of the complex with DNA as shown in (Fig. 25).

Conclusion

In this work, the nature of the interaction between the Eu(III) - TNB and DNA or nucleosides adenosine, guanosine, cytidine and inosine was studied. A method is presented for determination of nucleosides using the effect of enhancement of fluorescence of the easily accessible europium(III)-TNB in presence of different nucleosides. A similar method for the determination of DNA based on the quenching of Eu(III)-TNP has been estaplished.The interaction of Eu(III)-TNB complex with nucleosides (NS) (guanosine, adenosine, cytidine, inosine) and DNA has been studied using normal and time-resolved luminescence techniques. Binding constants were determined at 293 K, 298 K, 303 K, 308 K and 313 K by using Benesi-Hildebrand equation. A thermodynamic analysis showed that the reaction is spontaneous with ΔG being negative. The enthalpy ΔH and the entropy ΔS of reactions were all determined. The formation of binary and ternary complexes of Eu (III) with nucleosides and TNB has been studied potentiometrically at (25.0±0.1) °C and ionic strength I= 0.1 mol.dm^{-3} (KNO_3). Initial estimates of the formation constants of the resulting species and the protonation constants of the different ligands used have been refined with the HYPERQUAD computer program. Electrochemical investigations for the systems under investigations has been carried out using cyclic voltammetry (CV), differential pulse polarography (DPP), and square wave voltammetry (SWV) on glassy carbon electrode in I=0.1 mol/L p-toluenesulfonate as supporting electrolyte.

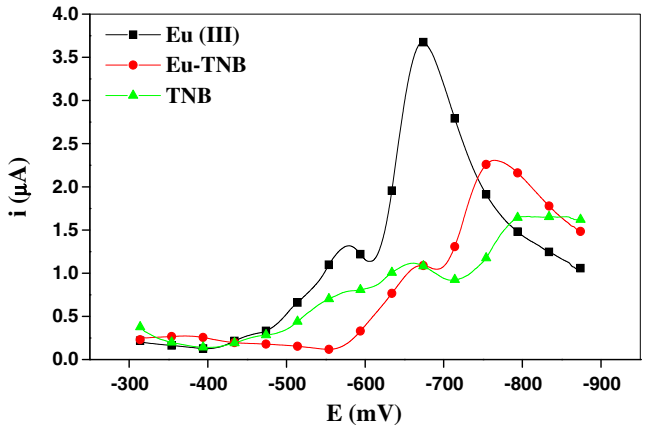

Fig. 23 Square wave voltammograms for the binary system Eu(III) - TNB in 0.1 M p-toluenesulfonate, frequency=20 Hz and at 25.0 °C [$C_{Eu}=1\times10^{-4}$ M, $C_{TNB}=2\times10^{-4}$ M]

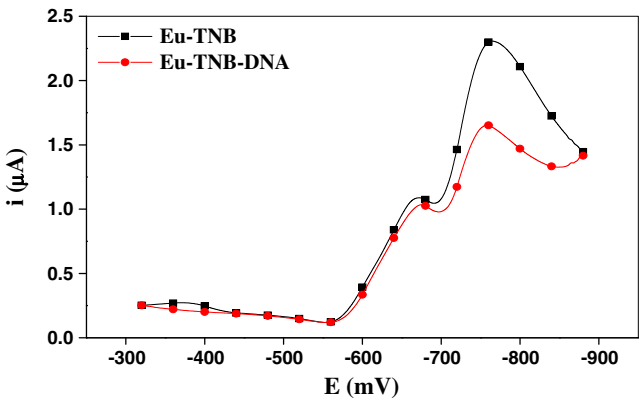

Fig. 25 Square wave voltammograms for the ternary system Eu(III)-TNB-DNA in 0.1 M p-toluenesulfonate, frequency=20 Hz, and at 25 °C. [$C_{Eu}=1\times10^{-4}$ M, $C_{TNB}=2\times10^{-4}$ M, and $C_{DNA}=1\times10^{-5}$ M]

References

1. Jiao K, Wang QX, Sun W, Jian FF (2005) Synthesis, characterization and DNA-binding properties of a new cobalt(II) complex: Co $(bbt)_2Cl_2$. J Inorg Biochem 99:1369–1375
2. Sigman DS, Graham DR, Aurora VD, Stern AM (1979) Oxygen-dependent cleavage of DNA by the 1,10-phenanthroline. cuprous complex. Inhibition of Escherichia coli DNA polymerase I. J Biol Chem 254:12269–12272
3. Yang ZS, Wang YL (2004) Electrochemically induced DNA cleavage by copper-bipyridyl complex. Electrochem Commun 6:158–163
4. Cater MT, Bard AJ (1987) Voltammetric studies of the interaction of tris(1,10-phenanthroline)cobalt(III) with DNA. J Am Chem Soc 109:7528–7530
5. Kawanishi S, Inoue S, Sano S (1986) Mechanism of DNA cleavage induced by sodium chromate(VI) in the presence of hydrogen peroxide. J Biol Chem 261:5952–5958
6. Chen QY, Li DH (1999) Interaction of a novel red-region fluorescent probe. Nile Blue, with DNA and its application to nucleic acids assay. Analyst 124:901–906
7. Li YF, Huang CZ, Huang XH (2001) Determination of DNA by its enhancement effect of resonance light scattering by azur A. Anal Chim Acta 429:311–319
8. Wang J, Xu D, Kawde AN, Polsky R (2001) Metal nanoparticle-based electrochemical stripping potentiometric detection of DNA Hybridization. Anal Chem 73:5576–5581
9. Wang H, Li WR, Lu Y, Fu NN, Zhang HS (2005) Vibrational frequencies and infrared intensities of the hydrogen-bonded complexes of nitrous acid with ethers: ab initio and DFT studies. Spectrochim Acta A 61:2103–2107
10. Zhang S, Zhong H, Ding C (2008) Chronocoulometric detection of DNA hybridization using reporter DNA probe modified with Au nanoparticles based on porous gold leaf electrode. Anal Chem 80:7206–7212
11. Zou QC, Yan QJ, Song GW, Zhang SL, Wu LM (2007) Detection of DNA using cationic polyhedral oligomeric silsesquioxane nanoparticles as the probe by resonance light technique. Biosens Bioelectron 22:1461–1465
12. Niu S, Singh G, Saraf RF (2007) Label-less fluorescence-based method to detect hybridization with applications to DNA microarray. Biosens Bioelectron 23:714–720
13. Fernandez MR, Gonzalez MJV, Garcia MED (1997) Room-temperature phosphorescent palladium–porphine probe for DNA determination. Anal Chem 69:2406–2410
14. Churchwell MI, Beland FA, Doerge DR (2002) Quantification of multiple DNA adducts formed through oxidative stress using liquid chromatography and electrospray tandem mass spectrometry. Chem Res Toxicol 15:1295–1301
15. Hason S, Pivonkova H, Vetter V, Fojta M (2008) Label-free sequence-specific DNA sensing using copper-enhanced anodic stripping of purine bases at boron-doped diamond electrodes. Anal Chem 80:2391–2399
16. Benedict JD, Forsham PH, Stetten D (1949) The metabolism of uric acid in the normal and gouty human studied with the aid of isotopic uric acid. J Biol Chem 181:183
17. Waslien CI, Calloway DH, Margen S (1968) Uric acid production of men fed graded amounts of egg protein and yeast nucleic acid. Am J Med 21:892
18. Griebsch A, Zollner N (1974) Effect of ribomononucleotides given orally on uric acid production in man. Adv Exp Med Biol 41:443
19. Garrel DR, Verdy M, PetitClerc C, Martin C, Bruke D, Hamet P (1991) Lowering of HDL2-cholesterol and lipoprotein A-I particle levels by increasing the ratio of polyunsaturated to saturated fatty acids. Am J Clin Nutr 53:665
20. Loffler W, Grobner W, Medina R, Zollner N (1982) Influence of dietary purines on pool size, turnover, and excretion of uric acid during balance conditions. Isotope studies using 15N-uric acid. Res Exp Med (Berl) 181:113
21. Yu TS, Berfe L, Gutman AB (1962) Renal function in gout. II. Efect of uric acid loading on renal excretion of uric acid. Am J Med 33:829
22. Choi HK, Liu S, Curhan G (2005) Intake of purine-rich foods, protein, and dairy products and relationship to serum levels of uric acid: the Third National Health and Nutrition Examination Survey. Arthritis Rheum 52:283
23. Harris MD, Siegel LB, Alloway JA (1999) Gout and hyperuricemia. Am Fam Physician 59:925
24. Gibson T, Rodgers AV, Simmonds HA, Court-Brown F, Todd E, Meilton V (1983) A controlled study of diet in patients with gout. Ann Rheum Dis 42:123
25. Faller J, Fox IH (1982) Ethanol-induced hyperuricemia: evidence for increased urate production by activation of adenine nucleotide turnover. N Engl J Med 307:1598
26. Cao G, Russel RM, Lischner N, Prior RL (1998) Serum antioxidant capacity is increased by consumption of strawberries, spinach, red wine or vitamin C in elderly women. J Nutr 128:2383
27. Yamaoka N, Kaneko K, Kudo Y, Aoki M, Yasuda M, Mawatari K, Yamada Y, Yamamoto T (2010) Analysis of purine in purine-rich cauliflower. Nucleos Nucleot Nucleic Acids 29:518
28. Clifford AJ, Riumallo JA, Young VR, Scrimshaw NS (1976) Effect of oral purines on serum and urinary uric acid of normal. Hyperuricemic and gouty humans. J Nutr 106:428
29. QianbT CZ, Yang MS (2004) Determination of adenosine nucleotides in cultured cells by ion-pairing liquid chromatography-electrospray ionization mass spectrometry. Anal Biochem 325:77
30. Cordell RL, Hill SJ, Ortori CA, Barrett DA (2008) Quantitative profiling of nucleotides and related phosphate-containing metabolites in cultured mammalian cells by liquid chromatography tandem electrospray mass spectrometry. J Chromatogr B 871:115
31. Cai Z, Song F, Yang MS (2002) Capillary liquid chromatographic-high-resolution mass spectrometric analysis of ribonucleotides. J Chromatogr A 976:135
32. Vela JE, Olson LY, Huang A, Fridland A, Ray AS (2007) Simultaneous quantitation of the nucleotide analog adefovir, its phosphorylated anabolites and 2′-deoxyadenosine triphosphate by ion-pairing LC/MS/MS. J Chromatogr B 848:335
33. Carli D, Honorat M, Cohen S, Megherbi M, Vignal B, Dumontet C, Payen L, Guitton J (2009) Simultaneous quantification of 5-FU, 5-FUrd, 5-FdUrd, 5-FdUMP, dUMP and TMP in cultured cell models by LCMS/MS. J Chromatogr B 877:2937
34. De Abreu RA, Van Baal JM, De Bruyn CH, Bakkeren JA, Schretlen ED (1982) Investigation of catecholamine metabolism using high-performance liquid chromatography. J Chromatogr 229:67
35. Klawitter J, Schmitz V, Klawitter J, Leibfritz D, Christians U (2007) Development and validation of an assay for the quantification of 11 nucleotides using LC/LC–electrospray ionization–MS. Anal Biochem 365:230
36. Gill BD, Indyk HE (2007) Determination of nucleotides and nucleosides in milks and pediatric formulas: a review. J AOAC Int 90:1354
37. Crauste C, Lefebvre I, Hovaneissian M, Puy JY, Roy B, Peyrottes S, Cohen S, Guitton J, Dumontet C, Perigaud C (2009) Validation and long-term evaluation of a modified on-line chiral analaytical method for therapeutic drug monitoring of (R, S)-methadone in clinical samples. J Chromatogr B 877:1417
38. Elbanovski M, Makowska B (1996) The lanthanides as luminescent probes in investigations of biochemical systems J. Photochem Photobiol A 99:85

39. Gudgin Dickson EF, Pollak A, Diamandis EP (1995) Time-resolved detection of lanthanide luminescence for ultrasensitive bioanalytical assays. J Photochem Photobiol B 27:3
40. Lis S, Elbanowski M, Makowska B, Hnatejko Z (2002) Energy transfer in solution of lanthanide complexes. Photobiology A 150:233
41. Azab HA, Anwar ZM, Ahmed RG (2010) Pyrimidine and purine mononucleotides recognition by trivalent lanthanide complexes with N-acetyl amino acids. J Chem Eng Data 55(1):459–475
42. Azab HA, El-Korashy SA, Anwar ZM, Hussein BHM, Khairy GM (2010) Synthesis and fluorescence properties of Eu-anthracene-9-carboxylic acid towards N-acetyl amino acids and nucleotides in different solvents. Spectrochim Acta A Mol Biomol Spectrosc 75:21–27
43. Azab HA, AboElNour KM, Sherif S (2007) Metal ion complexes containing di-, tripeptides and biologically important zwitterionic buffers. J Chem Eng Data 52:381–390
44. Azab HA, El-Korashy SA, Anwar ZM, Hussein BHM, Khairy GM (2010) Eu(lll)-anthracene-9-carboxylic acid as a responsive luminescent bioprobe and its electroanalytical Interactions with N-acetyl amino acids, nucleotides and DNA. J Chem Eng Data 55:3130–3141
45. Azab HA, Abd El-Gawad II, Kamel RM (2009) Ternary complexes formed by the fluorescent probe Eu (III)-9-anthracene carboxylic acid with pyrimidine and purine nucleobases. J Chem Eng Data 54:3069–3078
46. Filip W, Mojmir S, Li AX, Azab HA, Bartha R, Hudson RHE (2007) A robust and convergent synthesis of dipeptides-DOTAM conjugates as chelators for lanthanide ions: new PARACEST MRI agents. Bioconjug Chem 18(5):1625–1636
47. Orabi AS, Azab HA, ElDeghidy FS, Said H (2010) Ternary complexes of La(III), Ce(III), Pr(III) or Er(III) with adenosine 5'-mono,5'-di, and 5'-triphosphate as primary ligands and some biologically important zwitterionic buffers as secondary ligands. J Solution Chem 39:319–334
48. Azab HA, Al-Deyab SS, Anwar ZM, Gharib RA (2011) Fluorescence and electrochemical probing of N-acetylamino acids, nucleotides and DNA by Eu(lll) -bathophenanthroline complex. J Chem Eng Data 56(4):833–849
49. Azab HA, Al-Deyab SS, Anwar ZM, Kamel RM (2011) Potentiometric, electrochemical and fluorescence study of the coordination properties of the monomeric and dimeric complexes of Eu(lll) with nucleobases and PIPES. J Chem Eng Data 56:1960–1969
50. Azab HA, Al-Deyab SS, Anwar ZM, Abd El-Gawad II, Kamel RM (2011) Comparison of the coordination tendency of amino acids, Nucleobases or mononucleotides towards the monomeric and dimeric lanthanide complexes with biologically important compounds. J Chem Eng Data 56:2613–2625
51. Bates GR, Roy NR, Robinson AR (1964) Determination of pH: theory and practice. Wiley, New York
52. Gran G (1952) Determination of the equivalence point in potentiometric titration part II. Analyst 77:661
53. May PM, Williams DR (1985) Computational methods for the determination of Formation Constants. In: Leggett DJ (ed). Plenum Press, New York, pp. 37-70.
54. Bjerrum J (1941) Metal amine complex formation in aqueous solution. Haase, Copenhagen
55. Irving H, Rossotti HS (1953) Methods for computing successive stability constants from experimental formation curves. J Chem Soc 3397.
56. De Stefano C, Princi P, Rigano C, Sammartano S (1987) Computer analysis of equilibrium data in solution. ESAB2M: An improved version of the ESAB program. Ann Chim (Rome) 77:643
57. Gans P, Vacca AJ (1996) Investigation of equilibria in solution. Determination of equilibrium constants with the HYPERQUAD suite of programs. Talanta 43:1739
58. Kumar CV, Turner RS, Asunction EH (1993) Groove binding of a styrylcyanine dye to the DNA double helix: the salt effect. J Photochem Photobiol A Chem 74:231–238
59. Son GS, Yeo JA, Kim JM, Kim SK, Moon HR, Nam W (1998) Base specific complex formation of norfloxacin with DNA. Biophys Chem 74:225–236
60. Palu G, Valisena G, Ciarrocchi G, Gatto B, Palumbo M (1992) Quinolone binding to DNA is mediated by magnesium ions. Proc Natl Acad Sci USA 89:9671
61. Ocaña JA, Barragán FJ, Callejon M (2004) Fluorescence and terbium sensitised luminescence determination of garenoxacin in human urine and serum. Talanta 63:691
62. Teixeira LS, Grasso AN, Monteiro AM, Neto AMF, Vieira ND, Gidlund M, Courrol LC (2010) Enhancement on the europium emission band of europium chlortetracycline complex in the presence of LDL. Anal Biochem 400:19
63. Lakowicz JR (1999) Principles of fluorescence spectroscopy, 2nd edn. Plenum Press, New York, pp. 87, 95, 237–249, 331.
64. Benesi HA, Hildebrand JH (1949) Spectrophotometric investigation of the interaction of iodine with aromatic hydrocarbons. J Am Chem Soc 71:2703
65. Wei XF, Liu HZ (2000) The interaction between Triton X-100 and bovine serum albumin. Chin J Anal Chem 28:699
66. Kang J, Liu Y, Xie M, Li S, Jiang M, Wang Y (2004) Interactions of human serum albumin with chlorogenic acid and ferulic acid. Biochim Biophys Acta 1674:205
67. Ross PD, Subranmanian S (1981) Thermodynamics of protein association reactions-forced contributing to stability. Biochemistry 20:3096
68. Martin RB, Mariam YH (1979) Interactions between metal ions and nucleic bases, nucleosides, and nucleotides in solution. Met Ions Biol Syst 8:57
69. Martin RB (1985) Nucleoside sites for transition metal ion binding. Accounts Chem Res 18:32
70. Patterson GS, Holm RH (1972) Effects of chelate ring substituents on the polarographic redox potentials of tris(ß-diketonato)ruthenium(II, III) complexes. Inorg Chem 11:2285
71. Takeuchi T, Endo A, Shimizu K, Sato GP (1985) Electrochemical oxidation of tris(β-diketonato)-ruthenium(III) in acetonitrile solutions at platinum electrodes. J Electroanal Chem 185:185
72. Collman JP (1965) Reactions of metal acetylacetonates. Angew Chem Int Ed Engl 4:132
73. Brad AJ, Faulkner LR (1980) Electrochemical methods. Fundamentals and applications. Wiley, New York, 218
74. Oliveria-Brett AM, Piedade JAP, Silva LA, Diculescu VC (2004) Voltammetric determination of all DNA nucleotides. Anal Biochem 332:321
75. Neidle S, Balasubramanian S (2006) Quadruplex nucleic acids. RSC Publishing, Cambridge
76. Huppert JL (2008) Four-stranded nucleic acids: structure, function and targeting of G-quadruplexes. Chem Soc Rev 37:1375–1384
77. Burge S, Parkinson GN, Hazel P, Todd AK, Neidle S (2006) Quadruplex DNA: sequence, topology and structure. Nucleic Acids Res 34:5402–5415
78. Patel DJ, Phan AT, Kuryavyi V (2007) Human telomere, oncogenic promoter and 5'-UTR G-quadruplexes: diverse higher order DNA and RNA targets for cancer therapeutics. Nucleic Acids Res 35:7429–7455
79. Parkinson GN, Lee MP, Neidle S (2002) Crystal structure of parallel quadruplexes from human telomeric DNA. Nature 417:876–880
80. Haider S, Parkinson GN, Neidle S (2002) Crystal structure of the potassium form of an Oxytricha nova G-quadruplex. J Mol Biol 320:189–200
81. Haider SM, Parkinson GN, Neidle S (2003) Structure of a G-quadruplex-ligand complex. J Mol Biol 326:117–125

82. Phan AT, Kuryavyi V, Burge S, Neidle S, Patel DJ (2007) Structure of an unprecedented G-quadruplex scaffold in the human c-kit promoter. J Am Chem Soc 129:4386–4392
83. Schaffitzel C, Berger I, Postberg J, Hanes J, Lipps HJ, Plückthun A (2001) In vitro generated antibodies specific for telomeric guanine-quadruplex DNA react with Stylonychia lemnae macronuclei. Proc Natl Acad Sci USA 98:8572–8577
84. Paeschke K, Simonsson T, Postberg J, Rhodes D, Lipps HJ (2005) Telomere end-binding proteins control the formation of G-quadruplex DNA structures in vivo. Nat Struct Mol Biol 12:847–854
85. Oganesian L, Bryan TM (2007) Physiological relevance of telomeric G-quadruplex formation: a potential drug target. Bioessays 29:155–165
86. De Cian A, Grellier P, Mouray E, Depoix D, Bertrand H, Monchaud D, Teulade-Fichou MP, Mergny JL, Alberti P (2008) Plasmodium telomeric sequences: structure, stability and quadruplex targeting by small compounds. Chembiochem 9:2730–2739
87. Balasubramanian S, Neidle S (2009) G-quadruplex nucleic acids as therapeutic targets. Curr Opin Chem Biol 13:345–353
88. Baraldi PG, Tabrizi MA, Preti D, Fruttarolo F, Avitabile B, Bovero A, Pavani G, Carretero MCN, Romagnoli R (2003) DNA minor-groove binders. Design, synthesis, and biological evaluation of ligands structurally related to CC-1065, distamycin, andanthramycin. Pure Appl Chem 75:187–194